



# A Critical Review of the Evaluation of SiO<sub>2</sub>-Incorporated TiO<sub>2</sub> Nanocomposite for Photocatalytic Activity

Alaa Nihad Tuama<sup>1</sup> · Ehssan Al-Bermany<sup>1</sup> · Raad Shaker Alnayli<sup>2</sup> · Khalid Haneen Abass<sup>1</sup> · Karar Abdali<sup>3</sup> · Muhammad Hasnain Jameel<sup>4</sup>

Received: 20 October 2023 / Accepted: 20 January 2024  
© The Author(s), under exclusive licence to Springer Nature B.V. 2024

## Abstract

The main aim of the present study was to determine the impact of the Silica (SiO<sub>2</sub>) on the photocatalytic activity of Titanium dioxide (TiO<sub>2</sub>) nano composite at various circumstance of preparation. Over the past few decades, there has been an increasing trend toward researching novel photocatalysts for water purification and protecting the environment from pollution. These organic pollutants have been degraded using various methods, including sophisticated heterogeneous photocatalysis (PHCs) using titanium dioxide (TiO<sub>2</sub>). One of the most promising technologies seems to be using a TiO<sub>2</sub> photocatalyst. An appropriate architecture that reduces electron loss during the excitation state and promotes the absorption of photons is necessary to maintain the high efficiency of the TiO<sub>2</sub> photocatalyst in heterogeneous PHCs reactions. The heterogeneous PHCs under UV–visible solar light must be significantly improved to further enhance the flow of photo-induced charge carriers during the excitation state. Recently, the intriguing and distinctive characteristics of binary oxide photocatalyst systems or silica (SiO<sub>2</sub>) doping have attracted much attention and have become a favorite subject of study for many scientific organizations. Compared to pure TiO<sub>2</sub>, the features of this SiO<sub>2</sub> doping were found to improve the photocatalytic (PHC) behavior by increasing the surface area of the TiO<sub>2</sub> photocatalyst system. Therefore, this work critically reviews the modification of TiO<sub>2</sub>/SiO<sub>2</sub> photocatalysts for pollutant degradation.

**Keywords** PHCs activity · TiO<sub>2</sub>/SiO<sub>2</sub> · Nanocomposite · Photovoltaic · Pollutant degradation

## Symbols and their corresponding description

PHCs Photocatalytics  
VB Valence band  
CB Conduction band

MOs Metal oxides  
NCs Nanocomposites  
PL Photoluminescence  
Eg Energy band gap

## Highlights

- PHCs using TiO<sub>2</sub>.
- Synergetic interaction of TiO<sub>2</sub> with SiO<sub>2</sub>.
- The most important obstacles and challenges in PHCs.
- Improved PHC performance.

✉ Ehssan Al-Bermany  
ehssan@uobabylon.edu.iq

<sup>1</sup> Department of Physics, College of Education for Pure Sciences, University of Babylon, Hillah 5001, Iraq

<sup>2</sup> Radiological Techniques Department, College of Health and Medical Techniques, Al-Mustaqbal University, 51001 Babylon, Iraq

<sup>3</sup> Iraq Ministry of Education, Baghdad, Iraq

<sup>4</sup> Department of Physics and Chemistry, Faculty of Applied Science and Technology (FAST), Universiti Tun Hussein Onn Malaysia, 84600 Muar, Johor, Malaysia

## 1 Introduction

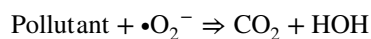
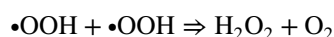
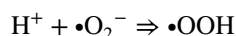
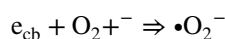
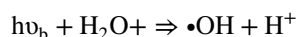
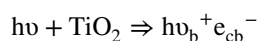
Over the past years, heterogeneous PHCs have been overgrown, particularly concerning energy and the preservation of the environment. Solar water splitting and the treatment of air and water with varying levels of contaminants have received the most research attention in PHCs. Numerous inorganic semiconductors, including SiO<sub>2</sub>, TiO<sub>2</sub>, and Cu<sub>2</sub>O, has been used in optoelectronics and photovoltaic application due to their exceptional electronic and physicochemical characteristics [1–3]. Due to their occupied valence band (VB) and unoccupied conduction band (CB) in the ground state, semiconductors typically function well as photosensitizers in PHC reactions. The formation of excitons, which are electrons at the CB and holes at the VB, respectively,

occurs when these semiconductors are triggered by energy larger than their band gap, resulting in PHCs. However, as shown in Fig. 1, the PHC effectiveness is typically influenced by two factors: (i) the poor quantum yield caused by rapid electron–hole ( $e^-_h+$ ) pair recombination, and (ii) the significant band gaps of semiconductors, which only allow for absorption in the UV area [4]. Therefore, numerous initiatives have been taken to enhance the effectiveness of PHCs of these materials. To increase these semiconductors' catalytic activity under UV and visible light, combining them with noble metals has proven to be one of the most efficient methods [5, 6]. These metal oxides (MOs) PHC activity is typically linked to non-selective free radical reaction mechanisms. They are, hence, frequently utilized to mediate the complete breakdown of these pollutants into  $\text{CO}_2$  and  $\text{H}_2\text{O}$  with  $\text{O}_2$  under UV irradiation, which is how organic contaminants in water are photodegraded.

Although titanium dioxide nanoparticles ( $\text{TiO}_2$  NPs) are a semiconductor photocatalyst that has been widely investigated, they have gained widespread acceptance due to their high catalytic efficiency, low cost, and simplicity of manufacture [7, 8].  $\text{TiO}_2$  is frequently used in a variety of applications, including the treatment of wastewater, dye-sensitized solar cells (DSSCs), lithium-ion batteries (electrodes), chemical sensing, and the production of hydrogen, antibacterial uses, and cosmetics [9–11].  $\text{TiO}_2$  lacks oxygen, making it an n-type semiconductor. Tetrahedral anatase, rutile, and orthorhombic brookite are three of its polymorphs. Due to the slow recombination of holes and electrons, anatase  $\text{TiO}_2$  NPs have the highest PHC activity. Anatase, rutile, and brookite have energy band gaps of 3.2, 3.0, and 3.2 eV, respectively [12–14]. Numerous studies show that the anatase and rutile phases in an appropriate ratio exhibit better PHC activity than anatase or rutile alone. Different techniques, including sol–gel, hydrothermal, or solvothermal, pulsed laser (PLD) deposition, chemical decomposition (CVD), chemical vapor decomposition, micelle and reversed micelle, direct oxidation, and sonochemical processes, can be used to create  $\text{TiO}_2$  NPs.

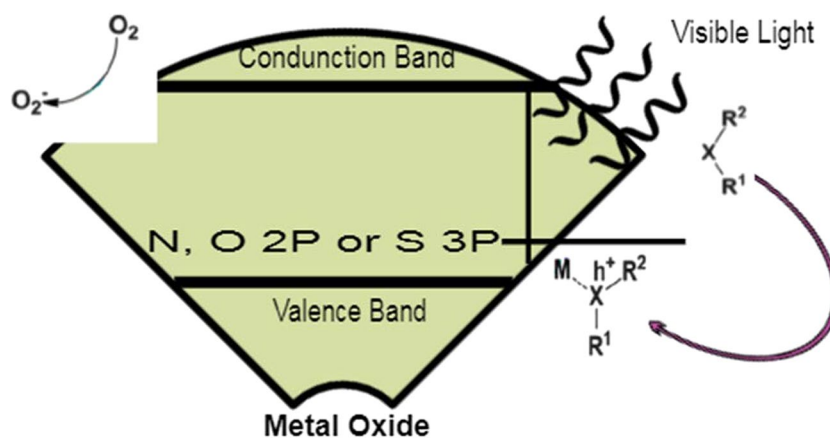
$\text{TiO}_2$  NPs have an advantage over other PHC semiconductors due to their photostability, low production costs, and chemical and biological inertness [15].

In PHCs, the three fundamental stages are light absorption, charge separation, and surface reaction. The excited electron transfers from the valence band to the conduction band when photons are stimulated by sunshine, which has photon energies equal to or greater than a photocatalyst's optical bandgap ( $E_g$ ). This process leaves a hole in the valence band, and "Charge separation" is the name given to this phenomenon. Reactive oxygen species (ROS), such as  $\bullet\text{O}_2$ ,  $\bullet\text{OH}$ , and  $\bullet\text{OOH}$ , which can remove contaminants from water and the air, can be created by the recombination or reaction of photogenerated electrons and holes with electron donors or acceptors. The most effective oxidizer of these ROS is OH, which is only surpassed by fluorine [16, 17]. The mechanism of the PHC process can be demonstrated by the following reactions [12]:



The reaction components are consumed and absorbed at the active sites of MO semiconductors ( $\text{TiO}_2$  NPs) in PHC

**Fig. 1** The electron–hole recombination of PHC efficiency in the MO semiconductors (original drawing by authors)



processes. The organization of the reactant surfaces and charge interchange between the TiO<sub>2</sub> NPs and pollutants causes the products to be generated on the surfaces of TiO<sub>2</sub> NPs. As a result, these products are desorbed and released into the environment. The resulting oxygen vacancies can also be photo-excited electron–hole pair separators, increasing the PHC activity. The emergence of unpaired electrons or Ti<sub>3</sub><sup>+</sup> centers due to the production of oxygen vacancies may result in the formation of donor levels in the TiO<sub>2</sub> electronic structure [18]. Different techniques, such as hydrogen thermal treatment, high-energy particle bombardment, doping of metals or non-metals, or thermal treatment under oxygen-depleted conditions, could produce defective TiO<sub>2</sub> with oxygen vacancies. Furthermore, a PHC activity might result in the formation of oxygen vacancies. However, charge recombination centers in high-density oxygen vacancies may reduce the mobility of free carriers and the effectiveness of PHCs [19, 20].

In addition to its benefits, TiO<sub>2</sub> NPs have three key drawbacks: rapid electron–hole pair recombination, poor light-source utilization, and challenging recycling [21]. Different techniques, such as linking with a narrower E<sub>g</sub> semiconductor, loading or co-loading with metal or non-metal, surface stimulation by metallic complexes or dyes made from organic material, coating of noble metals, top layer fluorination, and top layer sulfation, can be used to overcome the limitations of the large E<sub>g</sub> and the fast recombination of electron–hole pairs [22]. The limited recycling utility of TiO<sub>2</sub> NPs, which can cause issues with secondary contamination, is another restriction. TiO<sub>2</sub> NPs can be immobilized on various surfaces to overcome the recycling constraint. They also can be immobilized in a thermochemical, photochemical and electrochemical methods to minimize the contamination of toxic gases. Using only a small portion of the sample, thermogravimetric analysis (TGA) is a widely used method to comprehend the kinetic parameters of heat deterioration and the dominant response mechanism [23–27]. However, detachment of TiO<sub>2</sub> NPs from their carrier substrates by hydraulic blow and impact is a significant disadvantage of this approach [28]. However, immobilizing the photocatalyst in a matrix of TiO<sub>2</sub> like SiO<sub>2</sub> is one way to stop the release of TiO<sub>2</sub> from the surface into the environment. The earlier research on TiO<sub>2</sub>/SiO<sub>2</sub> nanocomposites (NCs) for diverse heterogeneous catalysis applications provides essential knowledge in this context [29–32]. However, another goal should be to create a mesoporous photocatalyst to enhance access to the active sites and, as a result, enhance catalytic activity. This can be done by developing mesostructured titania or adding TiO<sub>2</sub> to a matrix of mesoporous SiO<sub>2</sub> [33–35]. There are numerous techniques to integrate photoactive nanocrystalline TiO<sub>2</sub> particles into a mesoporous silica matrix: (1) by combining precursors of Si alkoxide and Ti alkoxide; (2) by gluing Ti alkoxide over

previously produced silica; or (3) by combining already-formed TiO<sub>2</sub> NPs colloidal with a solution of silicon alkoxide [36, 37].

However, challenges occur when Ti alkoxides are used because they hydrolyze much more quickly than Si alkoxides. Secondly, the amount of TiO<sub>2</sub> that can be loaded is relatively low. Third, the low heating temperature imposed by some substrates severely restricts the growth of photoactive TiO<sub>2</sub> crystals during a calcination process [29]. Grafting Ti alkoxide into the silica matrix necessitates the slow, laborious insertion of the alkoxides throughout multiple deposition cycles. Consequently, the creation of TiO<sub>2</sub>/SiO<sub>2</sub> NCs utilizing premade TiO<sub>2</sub> nanoparticles represents an intriguing possible alternative in various PHC processes, such as the purification of water and Atmospheric pollution [34]. Also, it was discovered that the catalyst films' thermal stability and mechanical strength are improved by the presence of SiO<sub>2</sub> [38]. Additionally, TiO<sub>2</sub> has a relatively high rate of electron–hole recombination, which is terrible for its photoactivity. Using different oxides when doping with SiO<sub>2</sub> could have two effects: First, by acting as electron traps, other oxides might lower the electron–hole recombination rate. Second, linking additional oxides could enhance the materials' physicochemical characteristics, such as their particular surface area, surface acidity, and surface hydroxyl [39]. Reviews of various aspects of TiO<sub>2</sub>/SiO<sub>2</sub> as a photocatalyst have been published in several publications. The new developments in several TiO<sub>2</sub>-based photocatalyst features are discussed in this research. The methods to prepare the TiO<sub>2</sub>/SiO<sub>2</sub>-based photocatalyst are discussed in the third section of this paper. The surface morphology of TiO<sub>2</sub>/SiO<sub>2</sub>-based photocatalyst is introduced in the fourth part, which also served as the primary topic of this review. TiO<sub>2</sub>/SiO<sub>2</sub> composite's PHC characteristics are examined in the fifth part.

## 2 Contribution of Metal oxides in enhancing PHCs

Numerous studies have been conducted on the electrical and optoelectronic properties of MOs such as ZnO, TiO<sub>2</sub>, and SiO<sub>2</sub> [40]. They have recently been demonstrated to operate as stable photocatalysts due to their exceptional electroactive capabilities and high electron–hole carrying. Studies on improving their processibility have also been extensively published [41, 42]. Table 1 displays the uses of a few samples of MO-based materials distinguished by various nanostructures. The table's listing of oxides is not all-inclusive, and the PHC abilities of MOs (TiO<sub>2</sub>/SiO<sub>2</sub>) will be covered in the following sections. From the findings in Table 1, it is clear that the structure of the core and functional components modulates the E<sub>g</sub> and surface adsorption

**Table 1** Examples of characteristic MO-based materials with diverse architectures

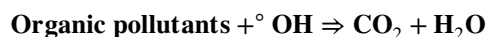
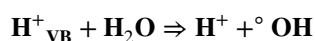
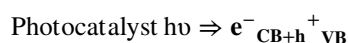
No	MO Material	Structural Properties	Approach to Synthesis	Application	Ref
1	Ag@SiO <sub>2</sub> /PVA-PEO	Core-shell structure	Casting	optoelectronic applications	[47]
2	Nanosheets of ZnO	floral-like 3D hierarchical structures	Solvothermal	Triphenylmethane dye adsorption	[48]
3	TiO <sub>2</sub> /SiO <sub>2</sub>	Core-shell	Sol-gel	Photodegrade-ion	[49]
4	TiO <sub>2</sub> /Cu <sub>2</sub> O	Heterostructure	Hydrothermal route	Water splitting	[50]
5	TiO <sub>2</sub> -Cu <sub>2</sub> O	Cubic structure	Electrochemical	PHCs	[51]
6	TiO <sub>2</sub> /ZnO	Spherical and hexagonal nanorods	Sol-gel	degradation of methyl orange	[52]
7	TiO <sub>2</sub> /Fe <sub>2</sub> O <sub>3</sub>	Hetero-structure	UV-assisted thermal synthesis	PHC degradation	[53]
8	TiO <sub>2</sub> /CdS	Core-shell	Microemulsion method	Visible Light PHC	[54]
9	ZnO-TiO <sub>2</sub> /clay	ZnO NPs with TiO <sub>2</sub> placed on a clay surface	Sol-gel method	Degradation of MG	[55]
10	TiO <sub>2</sub> /SiO <sub>2</sub>	Mesoporous amorphous	Sol-gel	Photodegrade -ion of quinoline	[56]

characteristics of these heterogeneous photocatalysts. For various MO applications,  $E_g$  modification, the structure of the material, and optoelectronic characteristics is essential [43–45]. The structural variation in MOs is produced by a variety of methods of synthesis, the most well-known of which include co-precipitation, deposition, hydrothermal technique, sol-gel method, sputtering, thermal evaporation, electrochemical deposition, soak-deoxidize-air oxidation, and impregnation [46].

Enhancing PHC activity involves doping with specific materials, manipulating shape, and having a high surface-to-volume ratio. Due to the high surface-to-volume ratio of nanomaterials, more surface area is available for redox reactions, increasing the PHC activity. Compared to their bulk counterpart, nanostructured materials have superior optical and chemical characteristics, indicating their function as photocatalysts [57]. In particular, gold nanoparticles exhibit chemical reactivity, whereas gold in bulk does not [58, 59]. In the form of nano-photocatalysts, zinc oxide (ZnO), titanium dioxide (TiO<sub>2</sub>), tungsten trioxide (WO<sub>3</sub>), copper oxide (CuO), tin dioxide (SnO<sub>2</sub>), and nickel oxide (NiO) have all been generated. These oxides' optical, chemical, and physical characteristics make them appropriate for various applications, including solar cells, catalysis, PHCs, antibacterial activity, and thermoelectricity. A few of the techniques used to make nano MOs have been described in the literature: vapor transport, co-precipitation, electrostatic spinning, hydrothermal, spray drying, sono-chemical synthesis, magnetron sputtering, sol-gel, and solution combustion [60].

The MO-based photocatalysts appear to do both ways that catalysts can change any reaction, lowering the activation energy and giving an alternative pathway for degrading dye and other organic pollutants. The three key phases that often make up the entire phenomena are separating the electron-hole charge carriers, distributing these charge carriers throughout the entire catalyst surface, and binding the

organic molecules to the active sites to advance the redox processes. The species that are most reactive in carrying out the degradation reaction are often H<sub>2</sub>O<sub>2</sub>, °OH, °OOH, and O<sub>2</sub>°-. Following is a description of how photocatalysts often aid in the degradation of organic molecules:



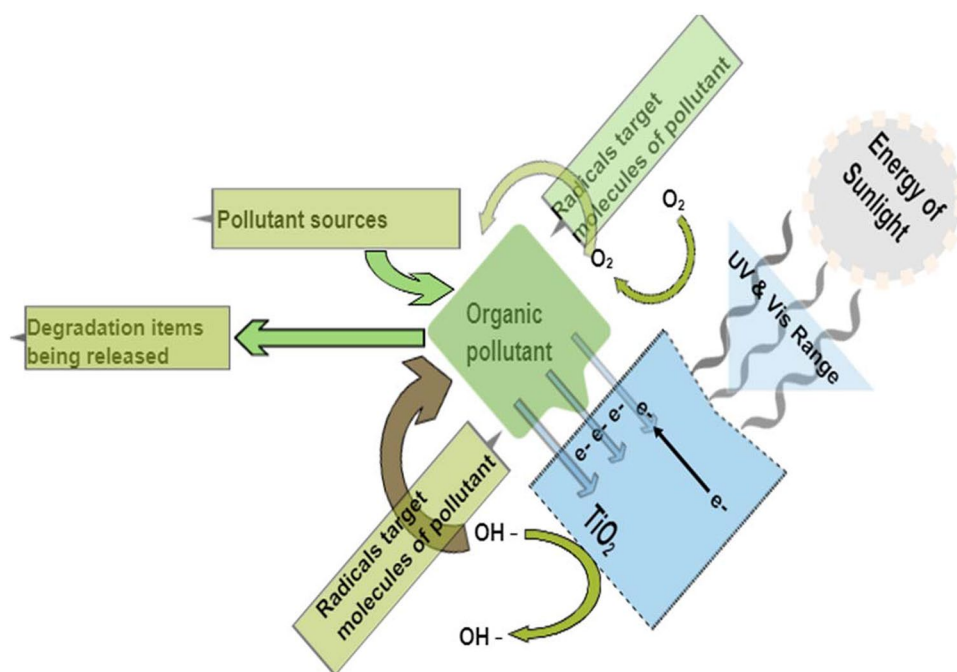
One of the best examples of this kind of catalyst that may release reactive radicals to target the organic pollutants (Fig. 2) present in an aqueous medium for an efficient degradation process is MO photocatalysts, such as TiO<sub>2</sub> [61, 62].

### 3 Properties of TiO<sub>2</sub>/SiO<sub>2</sub>

One of the fundamental properties of photocatalyst material is the band gap, which is directly related to the range of photon energies that may be used. TiO<sub>2</sub> can be used at the nanoscale or doped with SiO<sub>2</sub> to change or enhance its electrical, optical, and magnetic properties [63]. TiO<sub>2</sub> lends itself well to a wide range of daily applications without posing any concerns to human health or harming the environment because it is compatible with living beings [64]. When the TiO<sub>2</sub> is exposed to light, this causes the production of electron-hole pairs that can then react with oxygen or water to create highly reactive radicals that can degrade various organic and inorganic molecules.

SiO<sub>2</sub> is frequently utilized as a dopant distributed throughout the TiO<sub>2</sub> lattice or as a catalyst support. The

**Fig. 2** Diagram for TiO<sub>2</sub>-based pollution degradation (original drawing by authors)



essential characteristics of TiO<sub>2</sub> are impacted by this doping, which also impacts PHC activities. SiO<sub>2</sub>'s structural modification of TiO<sub>2</sub> dramatically increases TiO<sub>2</sub>-based photocatalyst's specific surface area. Due to its high porosity, TiO<sub>2</sub>/SiO<sub>2</sub> has a large surface area. High accessibility and diffusivity are made possible by the huge internal surface area per weight of high-porosity structures. As a result, contaminants are degraded more quickly on the surface of catalysts [65, 66]. The literature clearly shows that SiO<sub>2</sub> has improved the morphology of TiO<sub>2</sub>'s surface. According to Balachandran et al., the mean pore size derived from BET isotherms was 10 nm for TiO<sub>2</sub> and 15 nm for TiO<sub>2</sub>/SiO<sub>2</sub>, whereas the BET-specific surface area increased from 65 m<sup>2</sup> g<sup>-1</sup> for TiO<sub>2</sub> to 75 m<sup>2</sup> g<sup>-1</sup> for TiO<sub>2</sub>/SiO<sub>2</sub> [67].

There are two principal methods in charge of improving TiO<sub>2</sub> photoactivity. However, each TiO<sub>2</sub> alteration results in unique modifications in TiO<sub>2</sub>. The newly added elements to TiO<sub>2</sub> serve as traps for the photogenerated charge carriers, which lowers the rate of electron–hole pair recombination. The possibility that the electron–hole pairs will react with the species involved in the process is increased due to their longer lifetime, which boosts the photoprocess yield [68]. The newly formed photocatalysts have visible-range absorbance, enabling TiO<sub>2</sub> to be activated by visible light. Dopants are inserted into TiO<sub>2</sub> to change the structure and electronic structure, which results in a decrease in band-gap energy. Other materials, such as organic dyes or noble metal nanoparticles, absorb visible light and send their excited electron to the TiO<sub>2</sub>, starting the photo process.

#### 4 TiO<sub>2</sub>/SiO<sub>2</sub> Structure

TiO<sub>2</sub> has distinct crystal structures and typically exists in three polymorphs: tetrahedral anatase, rutile, and orthorhombic brookite. Due to the delay in recombining holes and electrons, anatase TiO<sub>2</sub> NPs have the highest PHC activity. Anatase, rutile, and brookite have energy E<sub>g</sub>s of 3.2, 3.0, and 3.2 eV, respectively [12, 14, 23]. This study shows that the combination of the anatase and rutile phases at a proper ratio has better PHC activity than anatase or rutile alone.

The overall particle size of TiO<sub>2</sub>/SiO<sub>2</sub> composite particles is reduced due to SiO<sub>2</sub> being deposited on TiO<sub>2</sub>. Balachandran et al. observed an absorption peak of maximum absorbance of TiO<sub>2</sub> and TiO<sub>2</sub>/SiO<sub>2</sub> at 372 and 352 nm, respectively, based on the spectra from the UV–Vis spectrophotometer. Due to the quantum confinement effect, the blue shift implies a reduction in particle size. Additionally, he stated that utilizing SEM and TEM analysis, pure TiO<sub>2</sub> displayed uneven morphological structure due to the aggregation of its particles and has an average diameter of 15–20 nm. TiO<sub>2</sub>/SiO<sub>2</sub> had a consistent shape and particles typically 7 to 10 nm in size [69, 70]. The typical particle size of TiO<sub>2</sub>/SiO<sub>2</sub> was 7–10 nm, displaying a uniform shape. This shows that the SiO<sub>2</sub>-modified TiO<sub>2</sub> photocatalyst comprises smaller particles with a higher surface area. The path of photoinduced electrons and holes used to move to the active sites on the TiO<sub>2</sub> surface is narrowed by the smaller size of TiO<sub>2</sub>/SiO<sub>2</sub> particles. TiO<sub>2</sub>/SiO<sub>2</sub> is a better photocatalyst than TiO<sub>2</sub> because it improves the efficiency of redox processes involving electrons and holes while decreasing the recombination rate of photoinduced electrons and holes.

According to Chengjun Ren et al., the microstrain of  $\text{TiO}_2/\text{SiO}_2$  samples elevated as the amount of  $\text{SiO}_2$  doping increased. The significant impact of the  $\text{SiO}_2$  dopant on the deformation of the anatase lattice can also be noted. As the  $\text{SiO}_2$  doping levels are increased, the  $\text{TiO}_2/\text{SiO}_2$  samples' crystallite sizes steadily decrease. The addition of Si to the anatase  $\text{TiO}_2$  lattice is thought to cause a decrease in crystallite size [40]. Additionally, the amorphous silica framework separates at the  $\text{TiO}_2$  grain boundary and prevents  $\text{TiO}_2$  species from forming big nanocrystals by preventing them from further coarsening and aggregating. Smaller particles can improve separation performance and decrease the combined photogenerated electric charge.

As A. Nilchi et al. reported, the anatase  $\text{TiO}_2$  crystallite size reduced from 9 to 5.09 nm. According to their findings,  $\text{SiO}_2$  doping into  $\text{TiO}_2$  might successfully slow nanoparticle formation and lower particle size. This observation could be explained by the creation of the Ti–O–Si link and the existence of amorphous  $\text{SiO}_2$  around the  $\text{TiO}_2$ , which would inhibit the growth of  $\text{TiO}_2$  particles [71].

## 5 Thermal Properties of $\text{TiO}_2/\text{SiO}_2$

Numerous factors, including pH, initial concentration, photocatalyst particle size and concentration, Thermal stability, light intensity, and electron acceptors, affect the PHC activity of materials. The overall thermal stability of  $\text{TiO}_2/\text{SiO}_2$  is increased by adding  $\text{SiO}_2$ , avoiding the transformation of anatase  $\text{TiO}_2$  into a rutile  $\text{TiO}_2$  crystal structure [30]. The link between the specific surface and pore volume of  $\text{TiO}_2$ , CTS-1 (Ti:Si 1), and CTS-4 (Ti:Si 4) and their different calcination temperatures was discussed by Wei et al. in their report [72]. The particular surface area of CTS-1 dropped from 437.4 to 176.3  $\text{m}^2 \text{g}^{-1}$ , and that of CTS-4 dropped from 309.5 to 121.2  $\text{m}^2 \text{g}^{-1}$  when the calcination temperature was raised from 500 to 950°C. The pore volume of CTS-1 changed from 1.39 to 0.52 ml  $\text{g}^{-1}$ , and that of CTS-4 changed from 0.55 to 0.30 ml  $\text{g}^{-1}$  when the calcination temperature was raised. As  $\text{SiO}_2$  increases, the thermal stability of  $\text{TiO}_2$ , CTS-1, and CTS-4 are less influenced by the rise in calcination temperature.

Mehran Riazian prepared a  $\text{TiO}_2/\text{SiO}_2$  nanopowder composite using the sol–gel method [73]. Due to the increasing surface area and thermal stability, adding low-composition  $\text{SiO}_2$  to the  $\text{TiO}_2$  matrix (less than 45%) improves the PHC activity.  $\text{SiO}_2$  oxides can have an impact on  $\text{TiO}_2$  by enhancing the thermal stability of anatase, inhibiting particle aggregation and anatase grain development, and increasing the specific area of the rutile phase. Since doping molecules could shield  $\text{TiO}_2$  nanoparticles from agglomerating at calcination temperatures, the effect of dopants displays a stabilizing effect on anatase. A. Nilchi et al. [71] provided a

study on various  $\text{TiO}_2/\text{SiO}_2$  NCs made using a brand-new sol–gel technique. The anatase phase existed at all temperatures examined in a phase transition investigation of as-synthesized nanocomposite thermally treated up to 1100 °C. The tetrahedral coordination of  $\text{TiO}_2$  in the  $\text{SiO}_2$  matrix, the anatase phase, and the huge surface area of the generated NCs provide them with good PHC capabilities. For the degradation of the Congo Red (CR) azo dye, the PHC capabilities of the composites were compared. Additional research was also designed to assess the composite's catalytic performance against that of synthetic pure  $\text{TiO}_2$ . The outcomes showed that the composite in its as-prepared state is the most efficient.

$\text{TiO}_2/\text{SiO}_2$  composites were produced by Tugrul Cetinkaya et al. [74] as photocatalysts utilizing the hydrolysis of  $\text{TiCl}_4$  and a suspension of  $\text{TiO}_2$  made from the hydrolysis of  $\text{TiCl}_4$ . To examine the impact of calcination temperature on the phase change of  $\text{TiO}_2$  structure,  $\text{TiO}_2/\text{SiO}_2$  composites were dried at 70 °C and calcined at 400 °C and 600 °C. It can be shown that even at 600 °C, hydrolyzed  $\text{TiO}_2$  retains its calcined anatase structure. Because anatase structure exhibits a superior PHC effect than rutile  $\text{TiO}_2$  structure, it was sought after to get anatase structure to obtain photodegradation of organic molecules efficiently.  $\text{TiO}_2/\text{SiO}_2$  composite generated by  $\text{TiO}_2$  suspension synthesized by hydrolysis of  $\text{TiCl}_4$  and calcined at 600 C exhibited 40% PHC degradation of AO7 after 2 h under UV light, and Composites' PHC activity is standardized by surface area.

Lihong Wu et al. successfully developed  $\text{SiO}_2/\text{TiO}_2$  teardrop-shaped nanoparticles with a core–shell structure using the sol–gel process [75]. The teardrop-shaped  $\text{SiO}_2/\text{TiO}_2$  nanoparticles demonstrated excellent thermal stability according to the TGA analysis, and improved photocatalytic removal of MB following a three-hour calcination at 500 oC. The analysis of the degradation mechanism revealed that the photogenerated holes were more crucial to the oxidation of MB than the photoinjected electrons. Moreover, the  $\text{SiO}_2/\text{TiO}_2$  photocatalyst that formed in the shape of a teardrop demonstrated high stability and reusability.

## 6 Electrical and Optical Properties of $\text{TiO}_2/\text{SiO}_2$

$\text{TiO}_2$  has a direct band-gap of 3.2 eV at ambient temperature, a high exciton binding energy of 458.5 eV meV, and excellent electro-optical and electrochemical stability [13]. Chemically, thermally, and when exposed to high-energy radiation,  $\text{TiO}_2$  is exceedingly stable. Wide direct band gap, increased electron mobility, high breakdown voltages, and increased breakdown field strength are all characteristics of the n-type  $\text{TiO}_2$  semiconductor [19]. Table 2 lists the optical and electrical characteristics of single-crystal  $\text{TiO}_2$ . Due to its superior electrical

**Table 2** Single crystal TiO<sub>2</sub>'s optical and electrical characteristics

Properties	Values	Ref
Energy gap ( $E_g$ )	3–3.2 eV (Direct)	[9]
Exciton binding energy	458–529 eV	[13]
Effective electron mass ( $m_e^*$ )	0.0948 $m_e/m_0$	[22]
Effective hole mass ( $m_h^*$ )	0.099 $m_h/m_0$	[78]
At 300 K, electron Hall mobility	18.6 $\text{cm}^2\text{V}^{-1}\text{s}^{-1}$	[79]
Refractive index	2.8736	[80]
Optical transmission, T (1/a)	90–95%	[81]
Carrier concentration	$1 \times 10^{16} \text{ cm}^{-3}$ to $1 \times 10^{20} \text{ cm}^{-3}$	[82]

properties, TiO<sub>2</sub> has been employed primarily in high-powered electronic devices, including field emission devices and photocatalyst applications [76]. Despite the advantages listed above, the main obstacle to creating self-cleaning materials based on TiO<sub>2</sub> is its absorption, which is only present in the UV spectrum. Numerous techniques have been employed to increase the PHC activity of TiO<sub>2</sub> and, as a result, the absorption of visible light, including alterations, doping, semiconductor linking, and dye sensitization. In addition to being unable to absorb visible light, TiO<sub>2</sub> has a quick recombination of the photogenerated electron–hole pairs ( $e^-/h^+$ ), a characteristic of all semiconducting materials [77]. As a result, these photogenerated charges need traps to serve as a reservoir, which slows down their rapid recombination. The visible range absorption and electron/hole recombination limitations should be considered while choosing the suitable material and method for titania modification. Due to SiO<sub>2</sub>'s excellent efficacy as a co-catalyst of titanium dioxide is one of the oxides utilized most frequently for TiO<sub>2</sub> modification. As a result, much research has been concentrated on it.

M. Vishwas et al. investigated the optical and electrical characteristics of TiO<sub>2</sub>/SiO<sub>2</sub> films developed via a practical sol–gel method [83]. While the reflectance of TiO<sub>2</sub> films fell as SiO<sub>2</sub> concentration increased, the optical transmittance of the same films increased. As SiO<sub>2</sub> concentration increased, the refractive index dropped. At 5 V, the current density and resistivity were determined to be  $2.26 \times 10^{-6} \text{ A/cm}^2$  and  $2.04 \times 10^{11} \text{ }\Omega\text{cm}$ , respectively, and the dielectric constant was found to be 3.45. It is appropriate for optoelectronic applications given the films' excellent optical transparency, shallow leakage current, and high dielectric constant.

## 7 TiO<sub>2</sub>/SiO<sub>2</sub>'s Luminescence and Lattice Dynamical Characteristics

Photoluminescence (PL) can be used to analyze the luminescence characteristics of TiO<sub>2</sub>. The UV-emission and broad visible emission areas represent the two regions of the PL

spectra that the TiO<sub>2</sub> nanostructure typically displays. In this instance, the repeated pairing of excitons (also known as band-to-band recombine) is responsible for the UV emission, also known as deep-level emission [76]. High crystalline TiO<sub>2</sub> would result in very high UV emission [77]. Different impurities and flaws are thought to cause the green band in the visible region of TiO<sub>2</sub>. The increase in visible emission intensity may be attributed to the high defect concentration caused by the recombination of electrons with oxygen vacancies and photoexcited holes in the valence band [84].

Raman spectroscopy analysis can determine the lattice dynamics of a single crystal of TiO<sub>2</sub>. Rutile, anatase with a tetragonal crystal lattice, and brookite with an orthorhombic crystal lattice are the three natural types of TiO<sub>2</sub>. The rutile phase, permanently converted by heat treatment at temperatures between 400 and 1200 C, is more thermodynamically stable than the anatase and brookite phases [85]. Rutile TiO<sub>2</sub>'s Lattice Dynamics and Raman Spectrum were investigated by Igor Lukacevic et al. [86]. They investigated the rutile phase of TiO<sub>2</sub>'s vibrational characteristics and Raman susceptibility tensor at low and high pressure. According to phonon simulations utilizing linear response theory, the rutile phase of TiO<sub>2</sub> has a phase transition below 10 GPa and is dynamically unstable at high pressures as shown in Fig. 3. At 10 GPa, the lattice dynamical instability at the G point is already evident, whereas a definite instability arises at 18 GPa. The experimental findings are shown as squares. Most recent research findings suggested that the lattice modification caused by mixing TiO<sub>2</sub> with SiO<sub>2</sub> gives the TiO<sub>2</sub>/SiO<sub>2</sub> mixed oxide more activity than pure TiO<sub>2</sub> when utilized as a photocatalyst. The addition of SiO<sub>2</sub> strengthens anatase TiO<sub>2</sub>'s thermostability, and its specific area and PHC activity are also increased [87–89].

The photoluminescence spectroscopy of immobilized TiO<sub>2</sub>/SiO<sub>2</sub> photocatalysts was discussed by Sudheera Yaparathne et al. [35]. The strength of the fluorescence peak is dependent on the mixture of holes and electrons, and the photoluminescence spectra are used to measure the separation efficiency of holes and electrons in semiconductor materials. They discovered that SiO<sub>2</sub> insertion further decreased the catalyst's photoluminescence. Even though SiO<sub>2</sub> generally increases a catalyst's activity by preventing electron–hole recombination.

## 8 Surface Morphological Properties of TiO<sub>2</sub>/SiO<sub>2</sub>

The surface morphology,  $E_g$ , electron–hole recombination, absorption of photons, crystallite size, defect concentration, facets, etc., are the primary factors affecting TiO<sub>2</sub>'s PHC performance [90]. The material's exposed facets and surface

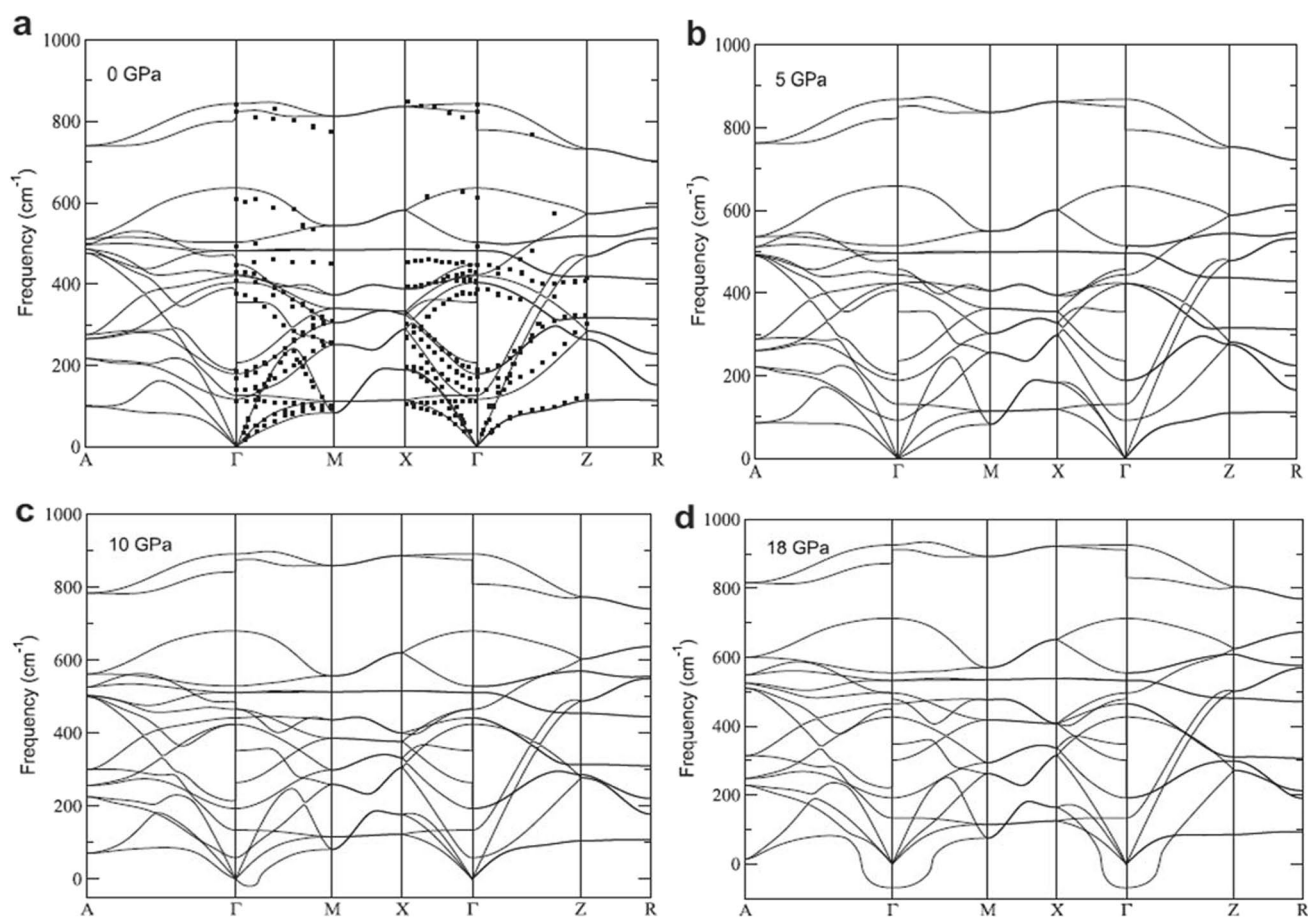


**Fig. 3** Four distinct phonon dispersion curves: (a) 0 GPa, (b) 5 GPa, (c) 10 GPa, and (d) 18 GPa [86]

characteristics have been found to play a significant role in determining PHC efficiency. Due to its capacity to handle energy and environmental challenges autonomously, semiconductor PHCs appear to be an emerging field of research.  $\text{TiO}_2$  has received the most research as a MO photocatalyst for various solar energy applications. Poor absorption wavelength, elevated charge carrier recombination, surface area, and other factors limit the  $\text{TiO}_2$  photocatalyst's performance [91, 92]. Various research has been conducted to overcome these limitations. One of these efforts was combining the  $\text{TiO}_2$  with  $\text{SiO}_2$ . Although  $\text{SiO}_2$  does not exhibit PHC properties, its high porosity and large specific surface area make it suitable as an adsorbent. Consequently, an increase in reactant concentration on the  $\text{TiO}_2$  surface can be assessed, improving the PHC activity of  $\text{TiO}_2$ . Moreover, the presence of  $\text{SiO}_2$  positively affects the enlargement of  $\text{TiO}_2$ -specific surface area. It also inhibits the phase change and grain growth of  $\text{TiO}_2$ . Overall, it enhances the PHC activity of  $\text{TiO}_2$ , confirming the synergistic role of silica in this type of composite and different substrates [93].

According to Balachandran et al. [69], who relied on data from the SEM and TEM investigation, pure  $\text{TiO}_2$  has an

average diameter of 15–20 nm. It exhibits an uneven morphological structure due to the aggregation of its particles.  $\text{TiO}_2/\text{SiO}_2$  had a consistent shape and particles, typically 7 to 10 nm in size. This demonstrates the smaller particles but more significant surface area of the  $\text{SiO}_2$ -modified  $\text{TiO}_2$  photocatalyst. The path of photoinduced electrons and holes used to move to the active sites on the  $\text{TiO}_2$  surface is narrowed by the smaller size of  $\text{TiO}_2/\text{SiO}_2$  particles.  $\text{TiO}_2/\text{SiO}_2$  is a better photocatalyst than  $\text{TiO}_2$  because it improves the efficiency of redox processes involving electrons and holes while decreasing the recombination rate of photoinduced electrons and holes.

Sudheera Yaparathne et al. reported on the Photodegradation of taste and odor compounds in water in the presence of immobilized  $\text{TiO}_2/\text{SiO}_2$  photocatalysts [35]. Increasing the Si content of the catalyst films reduces the formation of microcracks of the powder-modified films and brings about a higher robustness. Adding  $\text{SiO}_2$  to  $\text{TiO}_2$  nanoparticles has been found to minimize the aggregation of  $\text{TiO}_2$  particles, resulting in a better dispersion in the sol–gel mixture and less microcracks upon drying and calcination as illustrated in Fig. 4.

Nilchi et al. [71] evaluated the surface area and phase transformation with PHC activity of  $\text{TiO}_2/\text{SiO}_2$  composite samples. With increasing calcination temperature up to 1100 C, the surface area drops from 707.6 to 14.8  $\text{m}^2/\text{g}$ . The walls separating mesopores crystallize during calcination, which reduces the surface area. The surface area of pure  $\text{TiO}_2$  was likewise determined to be 90.4  $\text{m}^2/\text{g}$  for comparison's sake. As can be seen, the surface area of the  $\text{TiO}_2/\text{SiO}_2$  composite is significantly greater than that of pure  $\text{TiO}_2$  synthesized at the same temperature, demonstrating that  $\text{SiO}_2$  has modified the composite's overall surface area.

According to Tobaldi et al. [90], Dong et al. [91], adding  $\text{SiO}_2$  to  $\text{TiO}_2$  catalysts would result in smaller particles, a more significant amount of specific surface area, and a suppression of the  $\text{TiO}_2$  phase transition from anatase to rutile. Crystal size, surface acidity, and surface area of materials all significantly impact photoactivity. Precursors, methods

of preparation, and environmental factors are frequently responsible for altering the physicochemical properties.

## 9 Factors Influencing the Efficiency of Photodegradation

### 9.1 $\text{TiO}_2/\text{SiO}_2$ Loading

Most research reports have examined how catalyst loading affects PHC efficiency [74, 91, 92]. These findings showed that, until the desired mass was achieved, the photodegradation rate initially increased with increased catalyst loading. This phenomenon is predicated on the idea that increasing the catalyst dosage will increase the catalyst's overall active surface area and the number of reaction sites. Consequently, more hydroxyl and superoxide radicals were produced, which helped the organic contaminants degrade more

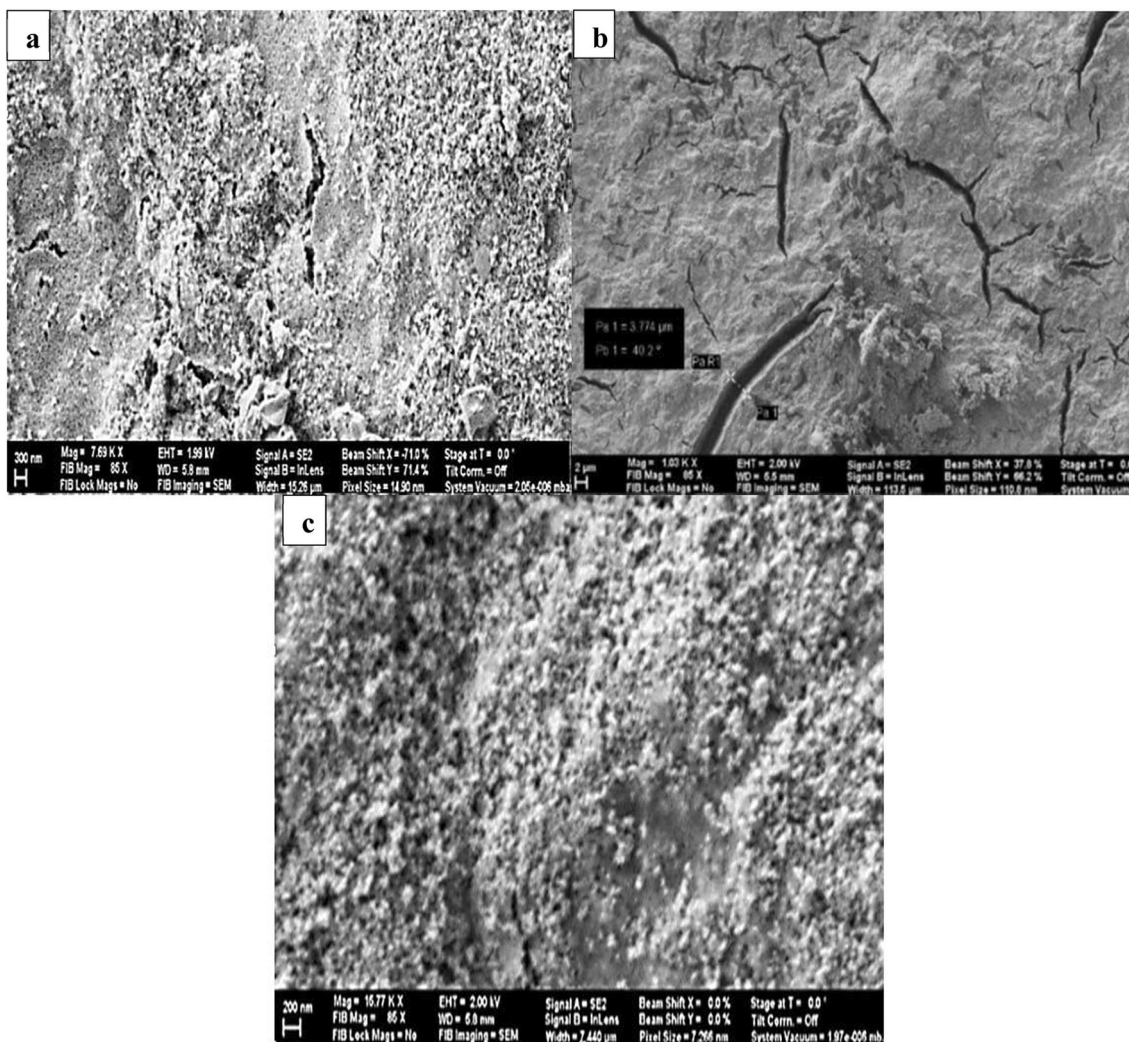


Fig. 4 The  $\text{TiO}_2/\text{SiO}_2$  photocatalyst films' SEM micrographs (High & Low Magnification) [35]

quickly. As a result, the deterioration percentage increased. However, when the photocatalyst dose was above the optimal concentration because of light scattering and screening effects, the percentage of photodegradation reduces at more significant loadings. Additionally, a high catalyst concentration promotes agglomeration (particle–particle contact), which reduces the amount of catalyst surface area accessible for light absorption and pollutant adsorption, lowering the PHC efficacy. On the other hand, it should be noted that the turbidity of the solution has also increased. This effect prevents light from entering the solution. Therefore, the suspension's photoactivated volume drops, which slows the degradation rate. These showed that to avoid using too much catalyst and to guarantee the maximal absorption of photons, the optimal catalyst mass should be attained.

## 9.2 Concentration of Substrate

Numerous studies have demonstrated that the rate of PHC degradation is adversely affected by the amount of organic pollutants present in aqueous solutions [93–96]. When the concentration of the substrate grew, the degradation efficiency decreased. This is because more and more organic compounds are adsorbed on the surface of the catalyst as the concentration of the target pollutant rises. As a result, the need for oxidizing species to degrade organic materials also rises. In addition, the photons get immobilized at increasing pollutant concentrations before they can reach the catalyst surface. The produced intermediates' competitive hydroxyl radical consumption lowers the degradation in the compelling contaminant solution.

## 9.3 PH of the Solution

The pH of the solution used in PHC water systems is crucial and impacts a semiconductor's conduction and valence bands in addition to the surface charge of the catalyst particles [97–105]. Additionally, the pH at which industrial wastewater is released can vary, complicating the PHC process. An organic chemical is often considered neutral when the pH of the solution is lower than its pKa value. The chemical deionizes and exists as a negatively charged species when the pH of the solution exceeds the pKa value. Additionally, the pH of the solution influences the electrostatic relationship between a catalyst surface, solvent molecules, substrate, and charged radicals produced in the photodegradation process.

The points of zero charge (pzc) for various semiconductors were reported by Kosmulski et al. [106]. Organic materials and the surface of the photocatalyst can be protonated and deprotonated under either acidic or alkaline circumstances. As a result, when the semiconductor surface is below its pzc value, it is positively charged; when it is above it, it is negatively charged. Shifu and Gengyu et al. [107]

claim that photogenerated holes (h) are the main oxidizing species in low pH environments. However, hydroxyl radicals primarily oxidize organic pollutants in neutral or alkaline environments. It should be highlighted, however, that high pH causes hydroxyl radicals to be quickly collected because numerous hydroxyl ions prevent their interaction with the substrate of the contaminant.

## 9.4 Intensity of Light

The rate of a PHC reaction relies on how much light a photocatalyst absorbs during the process. As light intensity increases, radiations fall on the catalyst surface and form more hydroxyl radicals, accelerating the reaction's pace. The amount of photoinduced holes in the valence band is significantly lower than that of photogenerated electrons in the conduction band in an n-type semiconductor like ZnO and TiO<sub>2</sub>. This demonstrated that the limiting active species are the photo-generated holes. The photodegradation rate and radiant flux are unrelated at significantly greater light intensities. The only factor affecting the response rate in this scenario is internal mass transfer. This is because both adsorption and desorption mass transfer are constrained. After all, the catalyst surface was entirely covered by saturated materials. Thus, despite increasing light intensity, the reaction rate does not change [11–109].

## 9.5 Temperature

Due to photonic activation, the process of PHC degradation can be used at room temperature and atmospheric pressure. The heating stage can be skipped during water treatment for water purification, which saves energy. With a few kJ/mol of activation energy, the ideal temperature for the PHC reaction is 20–80 °C.

## 10 PHC Activity of TiO<sub>2</sub>/SiO<sub>2</sub>

TiO<sub>2</sub>/SiO<sub>2</sub> composites are effective catalysts for a variety of chemical processes. As seen in the sections before, numerous studies on this composite have been conducted. The PHC activity of TiO<sub>2</sub>/SiO<sub>2</sub> is affected by several factors, as earlier discussed, and various research efforts have been devoted to highlighting the enhanced routes of this activity. When a suitable amount of SiO<sub>2</sub> is added to the TiO<sub>2</sub>/SiO<sub>2</sub> surface, the number of acidic sites increases, enhancing PHC activity. The development of more adsorption sites and the adsorption of more hydroxide ions are made more likely by an increase in surface acidic sites [110]. Inhibiting electron–hole recombination using hydroxide ions as "hole traps" results in a higher quantum yield. The TiO<sub>2</sub>/SiO<sub>2</sub>'s PHC activity is enhanced [111].

Additionally, it has been noted that the Ti/Si ratios significantly impact the PHC reactivity of TiO<sub>2</sub>/SiO<sub>2</sub> NCs. When considering the mechanical stability and the PHC activity, the optimal option appears to include roughly 50% SiO<sub>2</sub>.

Manuel Lunaa et al. have produced TiO<sub>2</sub>/SiO<sub>2</sub> photocatalysts with potential for use as construction materials that exhibit depolluting capability. SiO<sub>2</sub>-doped TiO<sub>2</sub> particles were used in the synthesis to produce sols that may be applied to construction materials using standard techniques. A PHC coating is made on the substrate surface of the building materials by the sols, which spontaneously gel to form TiO<sub>2</sub>/SiO<sub>2</sub> photocatalysts. The coating's activity is directly correlated with its TiO<sub>2</sub>/SiO<sub>2</sub> ratio. On the other hand, as the TiO<sub>2</sub> loading is elevated, the sol's viscosity rises, lowering substrate absorption and penetration [112].

Luis Pinho developed a unique and straightforward synthesis method for fabricating TiO<sub>2</sub>/SiO<sub>2</sub> photocatalysts on stones and other construction materials [113]. They showed that these photocatalysts have automatic cleanup characteristics on limestone that allowed them to stick to the stone securely and increase its durability. Furthermore, they concluded that this is a crucial variable for the effectiveness of the PHC activity. In particular, adding larger and sharper titania particles within a silica network significantly increased the efficiency of the photocatalyst on the stone, which improved its self-cleaning effect. Likewise, it has been demonstrated that the size and shape of the titania particles significantly influenced the PHC activity of the NCs created in this work. The excellent availability of photoactive surface locations in these materials was explained by improvement.

Employing immobilized TiO<sub>2</sub>/SiO<sub>2</sub> photocatalysts, Sudheera Yaparathne et al. investigated water's photodegradation of taste and odor components [35]. They created a TiO<sub>2</sub>/SiO<sub>2</sub> photocatalyst that increased UV activity without requiring particle catalysts to be removed using separation/filtration techniques. In drinking water and wastewater treatment plants, these catalyst films can supplement the current UV disinfection systems for removing taste and odor compounds and other organic contaminants.

TiO<sub>2</sub>/SiO<sub>2</sub> PHC cement series has been developed by C. Mendoza et al. to study the photo-efficiency of four TiO<sub>2</sub> coatings and the impact of the SiO<sub>2</sub> interlayer on the mechanic and PHC activity in Rhodamine B (RhB) and NO<sub>x</sub> photodegradation [114]. According to the study, all the PHC samples demonstrated strong photodegradation activity for RhB and NO<sub>x</sub>, with almost complete RhB molar transformations after five days of exposure and higher 53% for NO<sub>x</sub> photodegradation in an ongoing flow experiment. However, even though the commercial TiO<sub>2</sub> coatings were not stabilized by the SiO<sub>2</sub> layer deposited between mortar and photocatalysts, a high adherence was

seen when applied joint to homemade titania sol, likely because of the interactions among SiO<sub>2</sub> and TiO<sub>2</sub> sols.

Fatimah et al. synthesized various TiO<sub>2</sub>/SiO<sub>2</sub> composite materials utilizing titanium isopropoxide and biogenic silica from bamboo leaves as the silica supplier [115]. The prepared composite had physicochemical properties that made them sound as photocatalysts. They showed that rising the amount of TiO<sub>2</sub> improves the titanium dioxide's specific surface area, volume of pores, and size of particles as demonstrated in Fig. 5. At the same time, the band gap energy increases to a maximum of 3.21 eV for 40% and 60% Ti content. Since the composites with 40 and 60% wt of TiO<sub>2</sub> indicated a higher degradation rate than TiO<sub>2</sub> in the presence and absence of H<sub>2</sub>O<sub>2</sub>, they showed PHC activity with the MB degradation with increasing PHC efficiency.

Mesoporous TiO<sub>2</sub> particles with a silica shell have been developed by Peter Nadrah et al. [116]. In the presence of 5 mass equivalents of macromolecules (starch and HA), the material demonstrated an elevated level of selectivity for the degradation of cationic model pollutants (RhB). When starch is present in the solution, TiO<sub>2</sub>/SiO<sub>2</sub> maintains a total RhB degradation efficiency, and when HA is present, only a partial degradation efficiency.

Esfandiar Pakdela successfully synthesized TiO<sub>2</sub> and TiO<sub>2</sub>/SiO<sub>2</sub> discriminating photocatalysts using the low-temperature sol-gel technique [117]. SiO<sub>2</sub>'s influence was seen near TiO<sub>2</sub> as having a greater specific surface area and raising the photocatalyst's surface acidity. SiO<sub>2</sub> ratio in the composite was increased, which improved the PHC efficiency. Additionally, they observed a clear improvement in color removal compared to pure TiO<sub>2</sub> was achieved by utilizing an equivalent molar ratio of the composite components. They verified silica in boosting anatase titanium dioxide's PHC effectiveness on textiles.

Qi Jiang et al. efficiently produced hollow, raspberry-like microspheres with PHC activity. [118] by adding TiO<sub>2</sub> particles to the surface of SiO<sub>2</sub> that resembles raspberries. Compared to the smooth solid SiO<sub>2</sub> microspheres, the composite microspheres with hierarchical and hollow structures demonstrated higher PHC performance. They concluded that the hollow and hierarchical microspheres are advantageous for increasing PHC activity.

According to Weiyang Dong et al. [119], patterned 2D hexagonal mesoporous TiO<sub>2</sub>/SiO<sub>2</sub> NCs with broad pore channels and particular surface areas play a synchronous function in coupled adsorption and PHC oxidation. Such mesoporous structures comprise anatase TiO<sub>2</sub> crystals and amorphous SiO<sub>2</sub> nanoscale matrixes, which combine to form singular composite walls and offer previously unheard-of regions for combined PHC oxidation and adsorption. SiO<sub>2</sub> nano-matrixes were found to be effective adsorbents, offering superior adsorption sites and concentrating organic pollutant particles. At the same time, anatase crystals act as

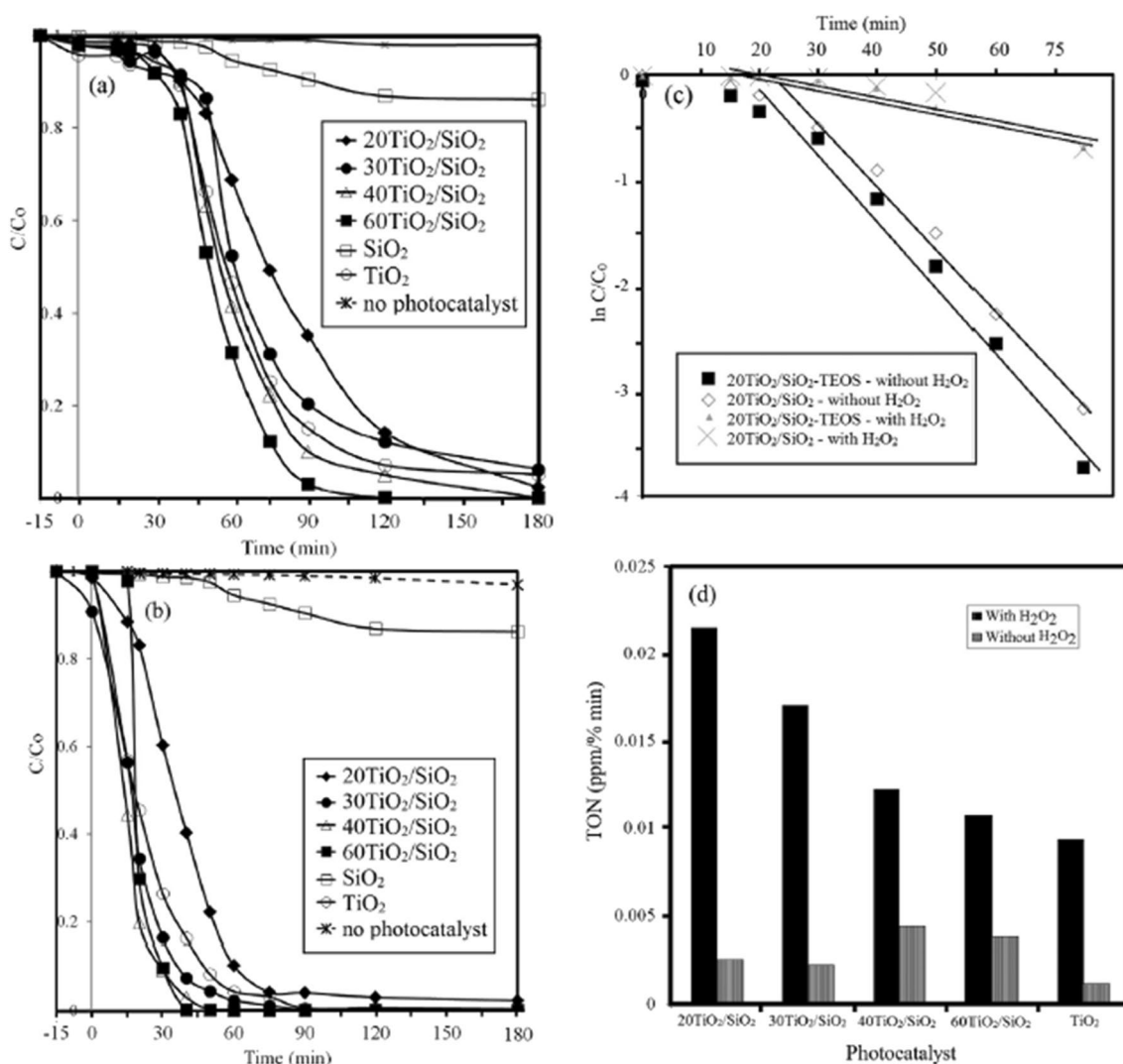


**Fig. 5** (a) The rate of photocatalytic degradation of MB without the inclusion of  $H_2O_2$ , (b) the MB photocatalytic rate with the inclusion of  $H_2O_2$ , (c) MB photocatalytic degradation pseudo-first

order plot of TiO<sub>2</sub>/SiO<sub>2</sub>, (d) Degradation over a variety of photocatalysts in the TON range [115]

PHC zones, oxidizing the organic molecules that the SiO<sub>2</sub> nanoparticles around them had already pre-enriched. Broad mesopore channels enable the reactive molecules to flow more freely into and out of the innermost surfaces before and after PHC reactions. In contrast, highly accessible surface areas can provide more adsorptive and PHCally active sites. Their method achieved the synchronous role by modifying the Ti/Si ratios, the number of surface hydroxyls, the size, and the crystallinity of the anatase nanocrystals on the particular composite frameworks. The obtained results showed that the synchronous role produces superb PHC activity.

In TiO<sub>2</sub>/SiO<sub>2</sub> composite coatings made and studied by Alejandra Romero et al., the effect of the crystalline shift and level of aggregates of TiO<sub>2</sub> nanoparticles incorporated in an amorphous SiO<sub>2</sub> matrix on PHC hydroxyl radical

formation and bacterial inactivation was established [120]. In the presence of hole, electron, oxide radical, and peroxide of hydrogen collectors that may be found in the bulk solution throughout wastewater treatment, the PHC hydroxyl radical production was investigated on TiO<sub>2</sub>/SiO<sub>2</sub> coatings. A relationship between the formation of hydroxyl radicals and a charge carrier transfer mechanism between defect concentrations in SiO<sub>2</sub> and TiO<sub>2</sub>-rooted nanoparticles has been established from the variability of rate parameters for hydroxyl radical growth in the appearance of each collector. By implementing the improved PHC activity of immobilized TiO<sub>2</sub> nanoparticles, their observation can be seen as an informative guide that would enable the processing of advanced PHC surfaces (which pose antimicrobial activity and antibacterial properties) that might be utilized throughout the

**Table 3** Various TiO<sub>2</sub>/SiO<sub>2</sub> nanocomposites that have been implemented as a photocatalyst

Contaminant	Conditions of the experiment	Findings based on degradation	Ref
Limestones and other building materials	The photocatalysts were sprayed as sols onto a construction limestone in a lab setting	The titania and silica particles' sizes and shapes are very important for the nanocomposites' photocatalytic activity	[112]
building materials (limestone, granite and concrete)	The photocatalysts were applied in a form of sols to building materials under solar radiation at dye degradation test	The activity of the coating is directly proportional to its TiO <sub>2</sub> /SiO <sub>2</sub> ratio. Raising the TiO <sub>2</sub> loading decreases absorption and penetration in the substrate by increasing the sol viscosity	[113]
Rhodamine B (Rh.B)	0.65 g L <sup>-1</sup> of untreated or treated TiO <sub>2</sub> nanoparticles and 0.025 g L <sup>-1</sup> were added to the aqueous dispersions	TiO <sub>2</sub> /SiO <sub>2</sub> nanoparticles appear to have a place in the self-clean coating materials	[118]
methyl isoborneol	Containing 200 mL quartz beakers with 500 ng L <sup>-1</sup> of MIB in deionized water (DI, 18 MΩ cm)	powder-modified catalyst films have the ability to photodegrade taste and odor compounds more efficiently than the UV-only treatment	[35]
Rhodamine B (RhB) and NOx	A 1.5 mL amount of 10–4 M RhB was applied to the mortar surfaces, and the samples were subsequently placed in the dark for a full day to enable the solution to dry and the dye to adsorb	Significant RhB and NOx photodegradation was seen in TiO <sub>2</sub> -SiO <sub>2</sub> , leading to nearly full RhB molar conversions and above 55% for NOx photooxidation, respectively	[114]
benzene	Gas phase photocatalytic oxidation with benzene was used in a 165 L handmade batch reactor to evaluate the photocatalytic activity of the TiO <sub>2</sub> /SiO <sub>2</sub> catalysts	The sample of TiO <sub>2</sub> /SiO <sub>2</sub> containing 5% SiO <sub>2</sub> and calcined at 650 °C exhibits the maximum benzene conversion when exposed to UV radiation at room temperature	[40]
Congo Red (CR) azo-dye	The reactor was a cylindrical glass container that held 300 mL of an aqueous CR (5 ppm) solution with 1 g/L of photocatalysts	On the surface of TSR, CR molecules are aggressively adsorbed and broken down, enabling more than 99% of the dye to be decolorized in 60 min	[71]
methylene blue, and NO	To study the photocatalytic activity and self-cleaning behavior of the photocatalysts on building materials, they were sprayed on concrete samples at room temperature	maximal methylene blue and soot destruction of 95% and 50% in 60 min and 168 h of radiation, respectively.	[80]
Methylene blue	500 mL of MB solution (20 mg L <sup>-1</sup> ) was usually mixed with 0.2 g of photocatalyst under the illumination of a UV lamp	Composites with 40 and 60% weight show increased photocatalytic efficiency and photocatalytic activity with MB degradation	[115]
acid orange	The concentration of acid orange 7 (AO7) was 5.0 ml with 62.59 × 10 <sup>-5</sup> M, whereas the concentration of photo-catalyst was 0.71 g/l	The TiO <sub>2</sub> /SiO <sub>2</sub> composite showed 40% photocatalytic destruction of AO7 after two hours under UV exposure, and the photocatalytic activity of the composites was normalized with surface area	[74]

disinfection phase of the treatment of wastewater. As a case study organic pollutant for PHC degradation using the TiO<sub>2</sub>/SiO<sub>2</sub> coupling system, methylene organic, a cationic dye, is frequently employed. Various types of degradation techniques such as adsorption, physicochemical degradation, photodegradation has been employed in the field of water-treatment. Four types of physicochemical processes—direct, indirect, photosensitized, and photocatalytic—occur in the atmosphere, water, and the uppermost layer of soil when exposed to radiation. The process of direct photodegradation involves molecules absorbing photons and converting them into higher energy levels by homolysis, heterolysis, or photolysis [121–124]. Table 3 lists the photocatalysis characteristics of SiO<sub>2</sub> incorporated TiO<sub>2</sub> nanocomposite at various preparation conditions and at various pollutant implementation.

## 11 Conclusions

The most promising photocatalyst for high PHC activity under UV, visible, and solar irradiation appears to be modified TiO<sub>2</sub>. According to several studies, reducing the possibility of charge carrier recombination rate is one of the most critical aspects that affect the PHC activity when utilizing the modified TiO<sub>2</sub> photocatalyst. Various modification techniques and chemical additions have been devised to reduce the recombination losses of charge carriers and expand TiO<sub>2</sub>'s spectral sensitivity to the visible spectrum. SiO<sub>2</sub> is often employed in this way as a dopant or catalytic support that is spread within the TiO<sub>2</sub> lattice. As a result of this doping's impact on TiO<sub>2</sub>'s fundamental characteristics, PHC activities are also impacted. The specific surface area of the TiO<sub>2</sub>-based photocatalyst is dramatically increased due to SiO<sub>2</sub>'s structural modification of TiO<sub>2</sub>. TiO<sub>2</sub>/SiO<sub>2</sub> is highly porous, which accounts for its high surface area. Excellent accessibility and diffusion are made possible by the substantial internal surface area per weight that high porosity structures possess. As a result, contaminants are degraded more quickly on the surface of catalysts. The reliable results would be a mechanistic understanding of basic science, which might be applied in pollution control via sophisticated PHC oxidation reactions to provide a clean-living environment for future generations.

**Acknowledgements** The authors thank the Department of Physics, University of Babylon, Iraq, for their support.

**Authors' Contributions** Alaa Nihad Tuama, Ehssan Al-Bermayn and Raad Shaker Alnayli suggested and designed the stature of the paper, Alaa Nihad Tuama wrote introduction section, Khalid Haneen Abass wrote the contribution of MOs in enhancing PHCs section and abstract, Karar Abdali wrote the properties of TiO<sub>2</sub>/SiO<sub>2</sub> and TiO<sub>2</sub>/SiO<sub>2</sub> structure sections and Muhammad Hasnain Jameel contributed to the thermal properties of TiO<sub>2</sub>/SiO<sub>2</sub>, Ehssan Al-Bermayn contributed to the

electrical and optical properties of TiO<sub>2</sub>/SiO<sub>2</sub> and TiO<sub>2</sub>/SiO<sub>2</sub>'s luminescence and lattice dynamical characteristics, and revised the whole paper. Alaa Nihad Tuama contributed to surface morphological properties of TiO<sub>2</sub>/SiO<sub>2</sub> and Factors influencing the efficiency of photodegradation, Raad Shaker Alnayli wrote PHC activity of TiO<sub>2</sub>/SiO<sub>2</sub> and conclusions. All authors reviewed all papers from scientific literature as they summarized the findings of existing literature, reviewed, read, and approved the final copy.

**Funding** No funding was applied.

**Data Availability** The data are available in the manuscript.

## Declarations

**Ethics Declarations** The manuscript does not involve any studies on humans or animals.

**Competing Interests** The authors declare no competing interests.

**Consent to Participate** Not applicable.

**Consent for Publication** Not applicable.

**Dual-Publication Statement** N/a.

## References

1. Abdali K (2022) Structural, Morphological, and Gamma Ray Shielding (GRS) Characterization of HVCMC/PVP/PEG Polymer Blend Encapsulated with Silicon Dioxide Nanoparticles. *Silicon* 14:9111–9116
2. Jabbar SA, Khalil SM, Abdulridha AR et al (2022) Dielectric, AC Conductivity, and Optical Characterizations of (PVA-PEG) Doped SrO Hybrid NCs. *Key Eng Mater* 936:83–92
3. Tuama AN, Abass KH, Agam MAB (2021) Efficiency enhancement of nano structured Cu<sub>2</sub>O: Ag/laser etched silicon-thin films fabricated via vacuum thermal evaporation technique for solar cell application. *Optik* 247:167980
4. Jakob M, Levanon H, Kamat PV (2003) Charge distribution between UV-irradiated TiO<sub>2</sub> and gold nanoparticles: determination of shift in the Fermi level. *Nano Lett* 3(3):353–358
5. Alawi AI, Al-Bermayn E, Alnayli RS, Sabri MM, Ahmed NM, Albermany AKJ (2024) Impact of SiO<sub>2</sub>-GO hybrid nanomaterials on opto-electronic behavior for novel glass quinary (PAAm-PVP-PVA/SiO<sub>2</sub>-GO) hybrid nanocomposite for antibacterial activity and shielding applications. *Opt Quant Electron* 56:429. <https://doi.org/10.1007/s11082-023-06070-3>
6. Tuama AN, Abbas KH, Hamzah MQ, Mezan SO, Jabbar AH, Agam MA (2020) An overview on characterization of silver/cuprous oxide nanometallic (Ag/Cu<sub>2</sub>O) as visible light PHC. *Int J Adv Sci Technol* 29(3):5008–5018
7. Ahlawat R, Srivastava VC, Mall ID, Sinha S (2008) Investigation of the electrocoagulation treatment of cotton blue dye solution using aluminium electrodes. *Clean-Soil, Air, Water* 36(10–11):863–869
8. Liu Z, Sun L, Zhang Q, Teng Z, Sun H, Su C (2022) TiO<sub>2</sub>-supported Single-atom Catalysts: Synthesis, Structure, and Application. *Chem Res Chin Univ* 38(5):1123–1138
9. Humayun M, Raziq F, Khan A, Luo W (2018) Modification strategies of TiO<sub>2</sub> for potential applications in PHCs: a critical review. *Green Chem Lett Rev* 11(2):86–102

10. Hamzah MQ, Jabbar AH, Mezan SO, Tuama AN, Agam MA (2019) Fabrications of PS/TiO<sub>2</sub> nanocomposite for solar cells applications. In AIP Conference Proceedings 2151(020011). <https://doi.org/10.1063/1.5124641>
11. Parrino F, Palmisano L (eds) (2020) Titanium dioxide (TiO<sub>2</sub>) and its applications. Elsevier, 1st edn. <https://doi.org/10.1016/C2019-0-01050-3>
12. Pelaez M, Nolan NT, Pillai SC, Seery MK, Falaras P, Kontos AG, Dionysiou DD (2012) A review on the visible light active titanium dioxide photocatalysts for environmental applications. *Appl Catal B* 125:331–349
13. Asahi R, Taga Y, Mannstadt W, Freeman AJ (2000) Electronic and optical properties of anatase TiO<sub>2</sub>. *Phys Rev B* 61(11):7459
14. Koelsch M, Cassaignon S, Minh CTT, Guillemoles JF, Jolivet JP (2004) Electrochemical comparative study of titania (anatase, brookite and rutile) nanoparticles synthesized in aqueous medium. *Thin Solid Films* 451:86–92
15. Zhang T, Liu Y, Rao Y, Li X, Yuan D, Tang S, Zhao Q (2020) Enhanced PHC activity of TiO<sub>2</sub> with acetylene black and persulfate for degradation of tetracycline hydrochloride under visible light. *Chem Eng J* 384:123350
16. Cunha DL, Kuznetsov A, Achete CA, da Hora Machado AE, Marques M (2018) Immobilized TiO<sub>2</sub> on glass spheres applied to heterogeneous PHCs: Photoactivity, leaching and regeneration process. *PeerJ* 6:e4464
17. Abdali K, Abass KH, Al-Bermany E et al (2022) Morphological, Optical, Electrical Characterizations and Anti-Escherichia coli Bacterial Efficiency (AECBE) of PVA/PAAm/PEO Polymer Blend Doped with Silver NPs. *Nano Biomed.* <https://doi.org/10.5101/nbe.v14i2.p114-122>
18. Nowotny MK, Sheppard LR, Bak T, Nowotny J (2008) Defect chemistry of titanium dioxide. Application of defect engineering in processing of TiO<sub>2</sub>-based photocatalysts. *J Phys Chem C* 112:5275–5300
19. Pan X, Yang MQ, Fu X, Zhang N, Xu YJ (2013) Defective TiO<sub>2</sub> with oxygen vacancies: synthesis, properties and PHC applications. *Nanoscale* 5(9):3601–3614
20. Katal R, Salehi M, Davood Abadi Farahani MH, Masudy-Panah S, Ong SL, Hu J (2018) Preparation of a new type of black TiO<sub>2</sub> under a vacuum atmosphere for sunlight PHCs. *ACS Appl Mater Interfaces* 10(41):35316–35326
21. Xing Z, Zhou W, Du F, Zhang L, Li Z, Zhang H, Li W (2014) Facile synthesis of hierarchical porous TiO<sub>2</sub> ceramics with enhanced PHC performance for micropolluted pesticide degradation. *ACS Appl Mater Interfaces* 6(19):16653–16660
22. Kumar SG, Devi LG (2011) Review on modified TiO<sub>2</sub> PHCs under UV/visible light: selected results and related mechanisms on interfacial charge carrier transfer dynamics. *J Phys Chem A* 115(46):13211–13241
23. Nawaz A, Mishra RK, Sabbarwal S, Kumar P (2021) Studies of physicochemical characterization and pyrolysis behavior of low-value waste biomass using Thermogravimetric analyzer: evaluation of kinetic and thermodynamic parameters. *Bioresour Technol Rep* 16:100858
24. Nawaz A, Kumar P (2022) Elucidating the bioenergy potential of raw, hydrothermally carbonized and torrefied waste *Arundo donax* biomass in terms of physicochemical characterization, kinetic and thermodynamic parameters. *Renew Energy* 187:844–856
25. Nawaz A, Kumar P (2022) Thermal degradation of hazardous 3-layered COVID-19 face mask through pyrolysis: Kinetic, thermodynamic, prediction modelling using ANN and volatile product characterization. *J Taiwan Inst Chem Eng* 139:104538
26. Nawaz A, Kumar P (2022) Pyrolysis behavior of low value biomass (*Sesbania bispinosa*) to elucidate its bioenergy potential: Kinetic, thermodynamic and prediction modelling using artificial neural network. *Renew Energy* 200:257–270
27. Nawaz A, Kumar P (2023) Impact of temperature severity on hydrothermal carbonization: Fuel properties, kinetic and thermodynamic parameters. *Fuel* 336:127166
28. Bui VKH, Park D, Pham TN, An Y, Choi JS, Lee HU, Lee YC (2019) Synthesis of MgAC-Fe<sub>3</sub>O<sub>4</sub>/TiO<sub>2</sub> hybrid NCs via sol-gel chemistry for water treatment by photo-Fenton and PHC reactions. *Sci Rep* 9(1):11855
29. Pénard AL, Gacoin T, Boilot JP (2007) Functionalized sol-gel coatings for optical applications. *Acc Chem Res* 40(9):895–902
30. Kibombo HS, Peng R, Rasalingam S, Koodali RT (2012) Versatility of heterogeneous PHCs: synthetic methodologies epitomizing the role of silica support in TiO<sub>2</sub> based mixed oxides. *Catal Sci Technol* 2(9):1737–1766
31. Kruk M, Jaroniec M, Sayari A (1997) Structural and surface properties of siliceous and titanium-modified HMS molecular sieves. *Microporous Mater* 9(3–4):173–182
32. Zhang W, Fröba M, Wang J, Tanev PT, Wong J, Pinnavaia TJ (1996) Mesoporous titanasilicate molecular sieves prepared at ambient temperature by electrostatic (S+ I-, S+ X-I+) and neutral (S° I°) assembly pathways: a comparison of physical properties and catalytic activity for peroxide oxidations. *J Am Chem Soc* 118(38):9164–9171
33. Alawi AI, Al-Bermany E (2023) Newly Fabricated Ternary PAAm-PVA-PVP Blend Polymer Doped by SiO<sub>2</sub>: Absorption and Dielectric Characteristics for Solar Cell Applications and Antibacterial Activity. *Silicon* 15:5773–5789
34. Oveisi H, Rahighi S, Jiang X, Nemoto Y, Beitollahi A, Wakatsuki S, Yamauchi Y (2010) Unusual antibacterial property of mesoporous titania films: drastic improvement by controlling surface area and crystallinity. *Chem-An Asian J* 5(9):1978–1983
35. Yaparathne S, Tripp CP, Amirbahman A (2018) Photodegradation of taste and odor compounds in water in the presence of immobilized TiO<sub>2</sub>/SiO<sub>2</sub> photocatalysts. *J Hazard Mater* 346:208–217
36. De Witte K, Meynen V, Mertens M, Lebedev OI, Van Tendeloo G, Sepulveda-Escribano A, Cool P (2008) Multi-step loading of titania on mesoporous silica: Influence of the morphology and the porosity on the catalytic degradation of aqueous pollutants and VOCs. *Appl Catal B* 84(1–2):125–132
37. Beyers E, Biermans E, Ribbens S, De Witte K, Mertens M, Meynen V, Cool P (2009) Combined TiO<sub>2</sub>/SiO<sub>2</sub> mesoporous photocatalysts with location and phase controllable TiO<sub>2</sub> nanoparticles. *Appl Catal B* 88(3–4):515–524
38. Suzuki N, Jiang X, Radhakrishnan L, Takai K, Shimasaki K, Huang YT, Yamauchi Y (2011) Hybridization of photoactive titania nanoparticles with mesoporous silica nanoparticles and investigation of their PHC activity. *Bull Chem Soc Jpn* 84(7):812–817
39. Kete M, Pavlica E, Fresno F, Bratina G, Štangar UL (2014) Highly active PHC coatings prepared by a low-temperature method. *Environ Sci Pollut Res* 21:11238–11249
40. Ren C, Qiu W, Chen Y (2013) Physicochemical properties and PHC activity of the TiO<sub>2</sub>/SiO<sub>2</sub> prepared by precipitation method. *Sep Purif Technol* 107:264–272
41. Abdali K (2023) Novel Flexible Glass Composite Film for Stretchable Devices Applications. *Silicon.* <https://doi.org/10.1007/s12633-023-02414-6>
42. Adnan MAM, Phoon BL, Julkapli NM (2020) Mitigation of pollutants by chitosan/metallic oxide photocatalyst: a review. *J Clean Prod* 261:121190
43. Danish MSS, Estrella LL, Alemaida IMA, Lysin A, Moiseev N, Ahmadi M, Senjyu T (2021) PHC applications of MOs for sustainable environmental remediation. *Metals* 11(1):80
44. Grilli ML, Chevallier L, Di Vona ML, Licocchia S, Di Bartolomeo E (2005) Planar electrochemical sensors based on YSZ with WO<sub>3</sub>

- electrode prepared by different chemical routes. *Sens Actuators, B Chem* 111:91–95
45. Aydoğan Ş, Grilli ML, Yilmaz M, Çaldıran Z, Kaçuş H (2017) A facile growth of spray based ZnO films and device performance investigation for Schottky diodes: determination of interface state density distribution. *J Alloy Compd* 708:55–66
  46. Attia AA, Hashim FS, Haneen Abass K (2023) Fabrication and characterization of p-Sb<sub>2</sub>O<sub>3</sub>:CuO/n-Si solar cell via thermal evaporation technique. *Int J Nanosci* 22:601–614. <https://doi.org/10.1142/S0219581X23500230>
  47. Lee KM, Lai CW, Ngai KS, Juan JC (2016) Recent developments of zinc oxide based photocatalyst in water treatment technology: a review. *Water Res* 88:428–448
  48. Guo T, Yao MS, Lin YH, Nan CW (2015) A comprehensive review on synthesis methods for transition-MO nanostructures. *CrystEngComm* 17(19):3551–3585
  49. Al-Bermany E, Mekhalif AT, Banimuslem HA et al (2023) Effect of green synthesis bimetallic Ag@SiO<sub>2</sub> core-shell nanoparticles on absorption behavior and electrical properties of PVA-PEO NCs for optoelectronic applications. *Silicon*. <https://doi.org/10.1007/s12633-023-02332-7>
  50. Pei C et al (2016) Superior adsorption performance for triphenylmethane dyes on 3D architectures assembled by ZnO nanosheets as thin as ~ 15 nm. *J Hazard Mater* 318:732–741
  51. Qourzal S, Barka N, Tamimi M, Assabbane A, Nounah A, Ihlal A, Ait-Ichou Y (2009) Sol-gel synthesis of TiO<sub>2</sub>-SiO<sub>2</sub> photocatalyst for β-naphthol photodegradation. *Mater Sci Eng, C* 29(5):1616–1620
  52. Wei T, Zhu YN, An X, Liu LM, Cao X, Liu H, Qu J (2019) Defect modulation of Z-scheme TiO<sub>2</sub>/Cu<sub>2</sub>O photocatalysts for durable water splitting. *ACS Catal* 9:8346–8354
  53. Li J, Liu L, Yu Y, Tang Y, Li H, Du F (2004) Preparation of highly PHC active nano-size TiO<sub>2</sub>-Cu<sub>2</sub>O particle composites with a novel electrochemical method. *Electrochem Commun* 6(9):940–943
  54. Liao DL, Badour CA, Liao BQ (2008) Preparation of nanosized TiO<sub>2</sub>/ZnO composite catalyst and its PHC activity for degradation of methyl orange. *J Photochem Photobiol, A* 194(1):11–19
  55. Nasirian M, Mehrvar M (2019) PHC degradation of aqueous methyl orange using a novel Ag/TiO<sub>2</sub>/Fe<sub>2</sub>O<sub>3</sub> photocatalyst prepared by UV-assisted thermal synthesis. *Desalin Water Treat* 137:371–380
  56. Lavand AB, Ys Malghe, Singh SH (2016) Synthesis, characterization and investigation of visible light photocatalytic activity of C, N Co-doped ZnO. *Adv Mater Lett* 7:181–186. <https://doi.org/10.5185/amlett.2016.5974>
  57. Tuama AN (2023) Thermally deposited silver-doped cuprous oxide solar cell on textured silicon and its devices modelling (Doctoral dissertation, Universiti Tun Hussein Onn Malaysia). <http://eprints.uthm.edu.my/id/eprint/8385>
  58. Yumak T, Bragg D, Sabolsky EM (2019) Effect of synthesis methods on the surface and electrochemical characteristics of MO/activated carbon composites for supercapacitor applications. *Appl Surf Sci* 469:983–993
  59. Ikram M, Rashid M, Haider A, Naz S, Haider J, Raza A, Maqbool M (2021) A review of PHC characterization, and environmental cleaning, of MO nanostructured materials. *Sustain Mater Technol* 30:e00343
  60. Di Paola A, García-López E, Marci G, Palmisano L (2012) A survey of PHC materials for environmental remediation. *J Hazard Mater* 211:3–29
  61. Hadjitaief HB, Zina MB, Galvez ME, Da Costa P (2016) PHC degradation of methyl green dye in aqueous solution over natural clay-supported ZnO-TiO<sub>2</sub> catalysts. *J Photochem Photobiol, A* 315:25–33
  62. Jesus MAML, Ferreira AM, Lima LFS, Batista GF, Mambrini RV, Mohallem NDS (2021) Micro-mesoporous TiO<sub>2</sub>/SiO<sub>2</sub> NCs: Sol-gel synthesis, characterization, and enhanced photodegradation of quinoline. *Ceram Int* 47(17):23844–23850
  63. Theerthagiri J, Chandrasekaran S, Salla S, Elakkiya V, Senthil RA, Nithyadharseni P, Kim HS (2018) Recent developments of MO based heterostructures for PHC applications towards environmental remediation. *J Solid State Chem* 267:35–52
  64. Akintelu SA, Folorunso AS, Folorunso FA, Oyebamiji AK (2020) Green synthesis of copper oxide nanoparticles for biomedical application and environmental remediation. *Heliyon* 6(7). <https://doi.org/10.1016/j.heliyon.2020.e04508>
  65. Aljaafari A (2022) Effect of metal and non-metal doping on the PHC performance of titanium dioxide (TiO<sub>2</sub>): a review. *Curr Nanosci* 18(4):499–519
  66. Peiris S, de Silva HB, Ranasinghe KN, Bandara SV, Perera IR (2021) Recent development and future prospects of TiO<sub>2</sub> PHCs. *J Chin Chem Soc* 68(5):738–769
  67. Liga MV, Maguire-Boyle SJ, Jafry HR, Barron AR, Li Q (2013) Silica decorated TiO<sub>2</sub> for virus inactivation in drinking water—simple synthesis method and mechanisms of enhanced inactivation kinetics. *Environ Sci Technol* 47(12):6463–6470
  68. Jeon H, Lee CS, Patel R, Kim JH (2015) Well-organized meso-macroporous TiO<sub>2</sub>/SiO<sub>2</sub> film derived from amphiphilic rubbery comb copolymer. *ACS Appl Mater Interfaces* 7(14):7767–7775
  69. Balachandran K, Venkatesh R, Sivaraj R, Rajiv P (2014) TiO<sub>2</sub> nanoparticles versus TiO<sub>2</sub>-SiO<sub>2</sub> NCs: A comparative study of photo catalysis on acid red 88. *Spectrochim Acta Part A Mol Biomol Spectrosc* 128:468–474
  70. Katoh R, Furube A, Yamanaka KI, Morikawa T (2010) Charge separation and trapping in N-doped TiO<sub>2</sub> photocatalysts: A time-resolved microwave conductivity study. *J Phys Chem Lett* 1(22):3261–3265
  71. Nilchi A, Janitabar-Darzi S, Mahjoub AR, Rasouli-Garmarodi S (2010) New TiO<sub>2</sub>/SiO<sub>2</sub> NCs—Phase transformations and PHC studies. *Colloids Surf, A* 361(1–3):25–30
  72. Wei Q, Li Y, Zhang T, Tao X, Zhou Y, Chung K, Xu C (2014) TiO<sub>2</sub>-SiO<sub>2</sub>-composite-supported catalysts for residue fluid catalytic cracking diesel hydrotreating. *Energy Fuels* 28(12):7343–7351
  73. Riazian M (2014) Dependence of PHC activity of TiO<sub>2</sub>/SiO<sub>2</sub> nanopowders. *J Nanostruct* 4(4):433–441
  74. Cetinkaya T, Neuwirthová L, Kutlákova KM, Tomášek V, Akbulut H (2013) Synthesis of nanostructured TiO<sub>2</sub>/SiO<sub>2</sub> as an effective photocatalyst for degradation of acid orange. *Appl Surf Sci* 279:384–390
  75. Wu L, Zhou Y, Nie W, Song L, Chen P (2015) Synthesis of highly monodispersed teardrop-shaped core-shell SiO<sub>2</sub>/TiO<sub>2</sub> nanoparticles and their photocatalytic activities. *Appl Surf Sci* 351:320–326
  76. Krasienapibal TS, Fukumura T, Hirose Y, Hasegawa T (2014) Improved room temperature electron mobility in self-buffered anatase TiO<sub>2</sub> epitaxial thin film grown at low temperature. *Jpn J Appl Phys* 53(9):090305
  77. Abdellatif S, Sharifi P, Kirah K, Ghannam R, Khalil ASG, Erni D, Marlow F (2018) Refractive index and scattering of porous TiO<sub>2</sub> films. *Microporous Mesoporous Mater* 264:84–91
  78. Diana M, Tasca M, Delibas M, Rusu GI (2000) On the structural properties and optical transmittance of TiO<sub>2</sub> rf sputtered thin films. *Appl Surf Sci* 156:200–206
  79. Sellers MC, Seebauer EG (2011) Measurement method for carrier concentration in TiO<sub>2</sub> via the Mott-Schottky approach. *Thin Solid Films* 519(7):2103–2110
  80. Khannayra S, Mosquera MJ, Addou M, Gil MLA (2021) Cu-TiO<sub>2</sub>/SiO<sub>2</sub> photocatalysts for concrete-based building

- materials: Self-cleaning and air de-pollution performance. *Constr Build Mater* 313:125419
81. Pallotti DK, Passoni L, Maddalena P, Di Fonzo F, Lettieri S (2017) Photoluminescence mechanisms in anatase and rutile TiO<sub>2</sub>. *J Phys Chem C* 121(16):9011–9021
  82. Wang J, Liu B, Nakata K (2019) Effects of crystallinity, {001}/ {101} ratio, and Au decoration on the PHC activity of anatase TiO<sub>2</sub> crystals. *Chin J Catal* 40(3):403–412
  83. Vishwas M, Rao KN, Gowda KA, Chakradhar RPS (2011) Optical, electrical and dielectric properties of TiO<sub>2</sub>-SiO<sub>2</sub> films prepared by a cost effective sol-gel process. *Spectrochim Acta Part A Mol Biomol Spectrosc* 83(1):614–617
  84. Komaraiah D, Radha E, Sivakumar J, Reddy MR, Sayanna R (2020) Photoluminescence and PHC activity of spin coated Ag<sup>+</sup> doped anatase TiO<sub>2</sub> thin films. *Opt Mater* 108:110401
  85. Serga V, Burve R, Krumina A, Pankratova V, Popov AI, Pankratov V (2021) Study of phase composition, PHC activity, and photoluminescence of TiO<sub>2</sub> with Eu additive produced by the extraction-pyrolytic method. *J Market Res* 13:2350–2360
  86. Lukačević I, Gupta SK, Jha PK, Kirin D (2012) Lattice dynamics and Raman spectrum of rutile TiO<sub>2</sub>: The role of soft phonon modes in pressure induced phase transition. *Mater Chem Phys* 137(1):282–289
  87. Feng H, Xu H, Feng H, Gao Y, Jin X (2019) The sol-gel synthesis and PHC activity of Gd-SiO<sub>2</sub>-TiO<sub>2</sub> photocatalyst. *Chem Phys Lett* 733:136676
  88. Jung SM, Grange P (2002) TiO<sub>2</sub>-SiO<sub>2</sub> mixed oxide modified with H<sub>2</sub>SO<sub>4</sub>: II. Acid properties and their SCR reactivity. *Appl Catal A: Gen* 228(1–2):65–73
  89. Czech B, Buda W (2015) Photocatalytic treatment of pharmaceutical wastewater using new multiwall-carbon nanotubes/TiO<sub>2</sub>/SiO<sub>2</sub> nanocomposites. *Environ Res* 137:176–184
  90. Gupta T, Cho J, Prakash J (2021) Hydrothermal synthesis of TiO<sub>2</sub> nanorods: for mation chemistry, growth mechanism, and tailoring of surface properties for PHC activities. *Mater Today Chem* 20:100428
  91. Dong H, Zeng G, Tang L, Fan C, Zhang C, He X, He Y (2015) An overview on limitations of TiO<sub>2</sub>-based particles for PHC degradation of organic pollutants and the corresponding countermeasures. *Water Res* 79:128–146
  92. Nair RG, Das A, Paul S, Rajbongshi B, Samdarshi SK (2017) MWCNT decorated V-doped titania: An efficient visible active photocatalyst. *J Alloy Compd* 695:3511–3516
  93. Rosales A, Esquivel K (2020) SiO<sub>2</sub>@ TiO<sub>2</sub> composite synthesis and its hydrophobic applications: a review. *Catalysts* 10(2):171
  94. Tobaldi DM, Tucci A, Škapin AS, Esposito L (2010) Effects of SiO<sub>2</sub> addition on TiO<sub>2</sub> crystal structure and PHC activity. *J Eur Ceram Soc* 30(12):2481–2490
  95. Dong W, Sun Y, Lee CW, Hua W, Lu X, Shi Y, ... Zhao D (2007) Controllable and repeatable synthesis of thermally stable anatase nanocrystal-silica composites with highly ordered hexagonal mesostructures. *J Am Chem Soc* 129(45), 13894–13904
  96. Xu G, Zheng Z, Wu Y, Feng N (2009) Effect of silica on the microstructure and PHC properties of titania. *Ceram Int* 35(1):1–5
  97. Wu A, Wang D, Wei C, Zhang X, Liu Z, Feng P, Niu J (2019) A comparative PHC study of TiO<sub>2</sub> loaded on three natural clays with different morphologies. *Appl Clay Sci* 183:105352
  98. Wu S, Tan X, Lei J, Chen H, Wang L, Zhang J (2019) Ga-doped and Pt-loaded porous TiO<sub>2</sub>-SiO<sub>2</sub> for PHC nonoxidative coupling of methane. *J Am Chem Soc* 141(16):6592–6600
  99. Teh CM, Mohamed AR (2011) Roles of titanium dioxide and ion-doped titanium dioxide on PHC degradation of organic pollutants (phenolic compounds and dyes) in aqueous solutions: A review. *J Alloy Compd* 509(5):1648–1660
  100. Murgolo S, Petronella F, Ciannarella R, Comparelli R, Agostiano A, Curri ML, Mascio G (2015) UV and solar-based PHC degradation of organic pollutants by nano-sized TiO<sub>2</sub> grown on carbon nanotubes. *Catal Today* 240:114–124
  101. Sood S, Umar A, Mehta SK, Kansal SK (2015) Highly effective Fe-doped TiO<sub>2</sub> nanoparticles photocatalysts for visible-light driven PHC degradation of toxic organic compounds. *J Colloid Interface Sci* 450:213–223
  102. Zhu J, Zäch M (2009) Nanostructured materials for PHC hydrogen production. *Curr Opin Colloid Interface Sci* 14(4):260–269
  103. Hisatomi T, Kubota J, Domen K (2014) Recent advances in semiconductors for PHC and photoelectrochemical water splitting. *Chem Soc Rev* 43(22):7520–7535
  104. Shi W, Fang WX, Wang JC, Qiao X, Wang B, Guo X (2021) pH-controlled mechanism of PHC RhB degradation over gC<sub>3</sub>N<sub>4</sub> under sunlight irradiation. *Photochem Photobiol Sci* 20:303–313
  105. Hu K, Li R, Ye C, Wang A, Wei W, Hu D, ... Yan K (2020) Facile synthesis of Z-scheme composite of TiO<sub>2</sub> nanorod/g-C<sub>3</sub>N<sub>4</sub> nanosheet efficient for PHC degradation of ciprofloxacin. *J Clean Prod* 253, 120055
  106. Kosmulski M (2006) pH-dependent surface charging and points of zero charge: III. Update. *J Colloid Interface Sci* 298(2):730–741
  107. Shifu C, Gengyu C (2005) PHC degradation of organophosphorus pesticides using floating photocatalyst TiO<sub>2</sub>·SiO<sub>2</sub>/beads by sunlight. *Sol Energy* 79(1):1–9
  108. Li X, Chen Y, Tao Y, Shen L, Xu Z, Bian Z, Li H (2022) Challenges of PHCs and their coping strategies. *Chem Catalysis* 2(6):1315–1345
  109. Rafiq A, Ikram M, Ali S, Niaz F, Khan M, Khan Q, Maqbool M (2021) PHC degradation of dyes using semiconductor photocatalysts to clean industrial water pollution. *J Ind Eng Chem* 97:111–128
  110. Cui L, Song Y, Wang F, Sheng Y, Zou H (2019) Electrospinning synthesis of SiO<sub>2</sub>-TiO<sub>2</sub> hybrid nanofibers with large surface area and excellent PHC activity. *Appl Surf Sci* 488:284–292
  111. Zhu Q, Pan D, Sun Y, Qi D (2022) Controllable Microemulsion Synthesis of Hybrid TiO<sub>2</sub>-SiO<sub>2</sub> Hollow Spheres and Au-Doped Hollow Spheres with Enhanced PHC Activity. *Langmuir* 38(13):4001–4013
  112. Luna M, Gatica JM, Vidal H, Mosquera MJ (2020) Use of Au/N-TiO<sub>2</sub>/SiO<sub>2</sub> photocatalysts in building materials with NO depolluting activity. *J Clean Prod* 243:118633
  113. Pinho L, Mosquera MJ (2013) PHC activity of TiO<sub>2</sub>-SiO<sub>2</sub> NCs applied to buildings: influence of particle size and loading. *Appl Catal B* 134:205–221
  114. Mendoza C, Valle A, Castellote M, Bahamonde A, Faraldos M (2015) TiO<sub>2</sub> and TiO<sub>2</sub>-SiO<sub>2</sub> coated cement: Comparison of mechanic and PHC properties. *Appl Catal B* 178:155–164
  115. Fatimah I, Prakoso NI, Sahroni I, Musawwa MM, Sim YL, Kooli F, Muraza O (2019) Physicochemical characteristics and PHC performance of TiO<sub>2</sub>/SiO<sub>2</sub> catalyst synthesized using biogenic silica from bamboo leaves. *Heliyon* 5(11). <https://doi.org/10.1016/j.heliyon.2019.e02766>
  116. Nadrah P, Gaberšček M, Škapin AS (2017) Selective degradation of model pollutants in the presence of core@ shell TiO<sub>2</sub>@ SiO<sub>2</sub> photocatalyst. *Appl Surf Sci* 405:389–394
  117. Pakdel E, Daoud WA, Seyedin S, Wang J, Razal JM, Sun L, Wang X (2018) Tunable PHC selectivity of TiO<sub>2</sub>/SiO<sub>2</sub> NCs: Effect of silica and isolation approach. *Colloids Surf, A* 552:130–141
  118. Jiang Q, Huang J, Ma B, Yang Z, Zhang T, Wang X (2020) Recyclable, hierarchical hollow photocatalyst TiO<sub>2</sub>@ SiO<sub>2</sub> composite microspheres realized by raspberry-like SiO<sub>2</sub>. *Colloids Surf, A* 602:125112
  119. Dong W, Lee CW, Lu X, Sun Y, Hua W, Zhuang G, Zhao D (2010) Synchronous role of coupled adsorption and PHC

- oxidation on ordered mesoporous anatase TiO<sub>2</sub>-SiO<sub>2</sub> NCs generating excellent degradation activity of RhB dye. *Appl Catal B* 95(3-4):197-207
120. Romero-Moran A, Sanchez-Salas JL, Molina-Reyes J (2021) Influence of selected reactive oxygen species on the photocatalytic activity of TiO<sub>2</sub>/SiO<sub>2</sub> composite coatings processed at low temperature. *Appl Catal B* 291:119685
121. Nawaz A, Singh B, Kumar P (2023) H<sub>3</sub>PO<sub>4</sub>-modified *Lagerstroemia speciosa* seed hull biochar for toxic Cr (VI) removal: isotherm, kinetics, and thermodynamic study. *Biomass Convers Biorefinery* 13(8):7027-7041
122. Zhu Y, Li H, Zhang G, Meng F, Li L, Wu S (2018) Removal of hexavalent chromium from aqueous solution by different surface-modified biochars: Acid washing, nanoscale zero-valent iron and ferric iron loading. *Biores Technol* 261:142-150
123. Jiahao W, Weiquan C (2020) One-step hydrothermal preparation of N-doped carbon spheres from peanut hull for efficient removal of Cr (VI). *J Environ Chem Eng* 8(6):104449
124. Mirabedini A, Mirabedini SM, Babalou AA, Pazokifard S (2011) Synthesis, characterization and enhanced photocatalytic activity of TiO<sub>2</sub>/SiO<sub>2</sub> nanocomposite in an aqueous solution and acrylic-based coatings. *Prog Org Coat* 72(3):453-460

**Publisher's Note** Springer Nature remains neutral with regard to jurisdictional claims in published maps and institutional affiliations.

Springer Nature or its licensor (e.g. a society or other partner) holds exclusive rights to this article under a publishing agreement with the author(s) or other rightsholder(s); author self-archiving of the accepted manuscript version of this article is solely governed by the terms of such publishing agreement and applicable law.